Set-Identification through Bounds on the Forecast Error Variance*†

Alessio Volpicella‡

PRELIMINARY DRAFT: January 2019

Abstract

Sign-restricted Structural Vector Autoregressions (SVARs) are increasingly common. However, they usually result in a set of structural parameters with very different implications in terms of impulse responses, elasticities, historical decomposition and forecast error variance decomposition (FEVD). This implies that it is hard to derive meaningful economic conclusions and there is the risk of retaining structural parameters with implausible implications. This paper proposes bounds on the FEVD to sharpen set-identification with sign restrictions. First, in a bivariate and trivariate setting, this paper analytically proves that bounds on the FEVD reduce the identified set. For higher dimensional SVARs, I establish conditions when placing bounds on the FEVD delivers a non-empty set and sharpens inference; correspondent algorithms to detect non-emptiness and reduction are provided. Second, under a convexity criterion, a prior-robust approach is proposed to construct estimation and inference. Third, this paper suggests a procedure to derive theory-driven bounds, consistent with the implications of popular DSGE models, with both real and nominal frictions, and with sufficiently wide ranges for their parameters. Fourth, a Monte-Carlo exercise documents effectiveness of those bounds to recover the data-generating process relative to sign restrictions. Finally, a monetary policy application shows that bounds on the FEVD (i) tend to remove unreasonable implications, sharpen and also alter the inference of models identified through sign restrictions and (ii) can be used for model validation.

Keywords: Sign Restrictions, Set Identification, Bounds, Forecast Error Variance, Structural Vector Autoregressions (SVARs), Monetary Policy.

JEL: C32, C53, E10, E52.

---

*I am indebted to Andrea Carriero and Haroon Mumtaz for invaluable guidance and support.

†I also thank Raffaella Giacomini, Christiane Baumeister, Dario Caldara, Toru Kitagawa, Wouter Den Haan, Matthias Meier, Emmanuel Guerre, Mathias Trabandt, Renato Faccini, Filippo Ferroni, Ron Smith, Konstantinos Theodoridis, George Kapetanios, Liudas Giraitis, Daniele Bianchi, Sylvain Barde, Emanuele Bacchiocchi, Mark Bognanni, Yuliya Lovcha and Alejandro Perez-Laborda for discussions and insightful suggestions. I would like to thank conference and seminar participants at the 12th International Conference on Computational and Financial Econometrics (CFE, University of Pisa), Empirical Macroeconomics seminar at Freie Universität Berlin, 71st European Meeting of the Econometric Society (ESEM, University of Cologne), 33rd Annual Congress of the European Economic Association (EEA, University of Cologne), 2018 International Association for Applied Econometrics annual conference (IAAE, Université du Québec à Montréal and Université de Montréal), 5th Money, Macroeconomics and Finance PhD conference (MMF PhD conference, University of Kent), and QMUL Reading Groups and PhD Conference for valuable comments and beneficial discussions. Financial support from Queen Mary University of London, School of Economics and Finance, and International Association for Applied Econometrics (IAAE) is gratefully acknowledged. All errors are mine.

‡Queen Mary University of London, School of Economics and Finance. Email: a.volpicella@qmul.ac.uk

1 Introduction and Related Literature

After Sims (1980), structural vector autoregressions (SVARs) are the common tool to study the dynamics caused by macroeconomic shocks. The early literature employs zero short-run, medium-run, or long-run restrictions on impulse response function (IRFs) for identification (Sims, 1980; Uhlig, 2004a; Blanchard and Quah, 1989). However, recent contributions relax controversial restrictions and attempt to rely on weaker assumptions. Specifically, since Faust (1998), Canova and Nicolo (2002), and Uhlig (2005), it is increasingly common to identify structural shocks with sign restrictions on either the impulse response functions or the structural parameters. Such restrictions are usually weaker than classical identification schemes and, as a result, likely to be agreed upon by researchers. Additionally, because the structural parameters and IRFs are set-identified, or bounded, conclusions are robust across the set of structural models that satisfy the sign restrictions. But this minimalist, or agnostic, approach comes at a cost. Sign restrictions will usually deliver a set of structural parameters with very different implications for IRFs, elasticities, historical decompositions, and forecast error variance decomposition (FEVD). On one hand, this makes obtaining informative inference and meaningful economic results challenging (Uhlig, 2005; Paustian, 2007; Mountford, 2005; Rafiq and Mallick, 2008; Arias, Caldara, and Rubio Ramírez, 2018; Antolín-Díaz and Rubio Ramírez, 2017; Amir-Ahmadi and Drautzburg, 2018). On the other hand, and even worse, some of the admissible structural models may contain implausible implications. Specifically, Kilian and Murphy (2012) find that sign restrictions on IRFs of a SVAR for the oil market induce highly questionable implications for the price elasticity of oil supply to demand shocks; more recently, Arias, Caldara, and Rubio Ramírez (2018) show that sign restrictions in Uhlig (2005) have counter-intuitive consequences for the systematic response of monetary policy; Antolín-Díaz and Rubio Ramírez (2017) argue that sign restrictions on IRFs for identification of oil and monetary policy shocks lead to implausible historical decomposition. Thus, the challenge is to come up with a small number of additional uncontroversial restrictions that help shrink the set of admissible structural parameters, eliminate unreasonable implications and allow us to reach clear economic conclusions.

While sign restrictions typically impose inequality constraints on the IRFs, this paper introduces bounds on the FEVD to sharpen identification, reduce the set of admissible structural parameters and remove implausible implications of sign-restricted models. In macroeconometrics, the FEVD is a very standard tool to evaluate if, and how much, shocks of interest explain unexpected fluctuations of target variables. The paper proposes to place theory-driven magnitude restrictions on the bounds of the FEVD and employ them as identifying constraints to sharpen set-identification induced by sign restrictions. Specifically, the paper makes the following contributions.

First, in a bivariate and trivariate setting, I analytically prove that bounds on the FEVD deliver a strictly smaller set relative to sign restrictions. Interestingly, this also applies to variables not subject to restrictions. For higher dimensional SVARs, I establish necessary conditions when placing bounds on the FEVD leads to a reduced identified set.

Second, the paper also addresses the trade-off between sharp identification and computation. In practice, it is unclear if the identification is sharp so that the identified set has a small, but positive, measure, or if the constraints are too tight and the set has zero measure (empty set).[1] As long as restrictions get tighter and reduce the identified set, it can be hard to distinguish between small and empty sets. Thus, this paper establishes sufficient conditions to determine whether the identified set has positive measure; a correspondent algorithm provides a computationally-fast practical check of the conditions. While recent studies (Giacomini and Kitagawa, 2018; Amir-Ahmadi and Drautzburg, 2018; Gafarov, Meier, and Olea, 2018) establish conditions for non-emptiness under zero and sign restrictions, this paper advances the literature by investigating non-emptiness under bounds on the FEVD.

The current state-of-the-art for Bayesian estimation and inference of sign-restricted models relies on drawing reduced-form parameters and an orthonormal matrix that maps the former into structural parameters, IRFs and any other object of interest (Arias, Rubio-Ramirez, and Waggoner, 2017). While the common approach is to impose a uniform distribution on the orthonormal matrix, it is well-known that (i) this choice does not imply a uniform distribution over the identified set of the structural parameters and (ii) the posterior of structural parameters is proportional to the prior distribution, even asymptotically (Baumeister and Hamilton, 2015). Under a convexity criterion, this paper presents a robust-prior procedure through a numerical optimizer, where the identified set, which is constrained by bounds on the FEVD, is distribution-free and does not depend on a specific prior over the orthonormal matrix. This is line with the proposals in Giacomini and Kitagawa (2018), Gafarov, Meier, and Olea (2018), and Amir-Ahmadi and Drautzburg (2018) for sign and zero restrictions only.

Once established that bounds on the FEVD help, we still need to find a way to choose a reasonable set of constraints in realistic settings. This leads to adapt the procedure in Canova and Paustian (2011) and derive theory-driven bounds on the FEVD, consistent with the implications of popular DSGE models, with both real and nominal frictions, and with sufficiently wide ranges for their parameters.

A Monte-Carlo exercise documents effectiveness of those bounds as identifying restrictions in recovering the data-generating process (DGP) relative to sign restrictions. While sign re-

[1] Uhlig (2017) summarises the trade-off as follows: "When a lot of draws are rejected, the identification is sharp".

strictions typically suggest that contractionary monetary policy shocks have no effects on real variables and are even likely to increase the real activity, an empirical application shows that bounds on the FEVD of inflation and interest rates tend to be highly informative, remove unreasonable effects of monetary shocks on real variables, and sharpen the inference of sign-restricted models. In doing so, the approach here is also more effective than alternative strategies of set-reduction, including long-run equality restrictions on the FEVD (Uhlig, 2004b), narrative sign restrictions (Antolín-Díaz and Rubio Ramírez, 2017), and ranking of IRFs (Amir-Ahmadi and Drautzburg, 2018). It also recovers reasonable signs for the coefficients of the monetary policy equation (Arias, Caldara, and Rubio Ramírez, 2018). Finally, the application also shows how to employ restrictions on the FEVD for model validation. As is clear, this paper's approach aims at reducing the dimension of the identified set from a sign-restricted SVAR. It does so by complementing sign restrictions with a completely novel methodology,[2] namely imposing constraints on the FEVD bounds.

The paper is organised as follows. Section 2 provides the econometric framework for set-identified SVARs. Section 3 introduces bounds on the FEVD, it analytically illustrates the reduction of the identified set in a bivariate and trivariate setting, it establishes conditions for non-emptiness and reduction for higher dimensional SVARs, and it delivers estimation and inference under constraints on the FEVD. Section 4 shows how to derive theory-driven bounds on the FEVD. Section 5 presents a Monte-Carlo experiment to investigate the performance of the identification through bounds on the FEVD. Section 6 provides the monetary policy application. Finally, Section 7 concludes.

2 The Econometric Framework

This Section defines the SVAR. It then introduces the identification problem and the class of standard equality and sign restrictions.

2.1 The Model

Consider a SVAR(p) model

$$\boldsymbol{A}_0\boldsymbol{y}_t = \boldsymbol{a} + \sum_{j=1}^{p} \boldsymbol{A}_j\boldsymbol{y}_{t-j} + \boldsymbol{\epsilon}_t \tag{2.1}$$

[2]The only exception is Dedola and Neri (2007). As robustness check, among the set of structural impulse vectors that satisfy sign restrictions, they select those that account for over 70% of the FEV of labour productivity to technology shock after 10 years. To my knowledge, I am the first to formalise the idea and develop the methodology.

for $t = 1, \ldots, T$, where $\boldsymbol{y}_t$ is an $n \times 1$ vector of endogenous variables, $\boldsymbol{\epsilon}_t$ an $n \times 1$ vector white noise process, normally distributed with mean zero and variance-covariance matrix $\boldsymbol{I}_n$, $\boldsymbol{A}_j$ for $j = 0, \ldots, p$ is an $n \times n$ matrix of structural coefficient. As usual in literature, structural disturbances are assumed to be uncorrelated. The initial conditions $\boldsymbol{y}_1, \ldots, \boldsymbol{y}_p$ are given. Let $\boldsymbol{\theta} = (\boldsymbol{A}_0, \boldsymbol{A}_+)$ collect the structural parameters, where $\boldsymbol{A}_+ = (\boldsymbol{a}, \boldsymbol{A}_j)$ for $j = 1, \ldots, p$. The reduced-form VAR is as follows

$$\boldsymbol{y}_t = \boldsymbol{b} + \sum_{j=1}^{p} \boldsymbol{B}_j \boldsymbol{y}_{t-j} + \boldsymbol{u}_t, \tag{2.2}$$

where $\boldsymbol{b} = \boldsymbol{A}_0^{-1}\boldsymbol{c}$ is an $n \times 1$ vector of constants, $\boldsymbol{B}_j = \boldsymbol{A}_0^{-1}\boldsymbol{A}_j$, $\boldsymbol{u}_t = \boldsymbol{A}_0^{-1}\boldsymbol{\epsilon}_t$ denotes the $n \times 1$ vector of reduced-form errors. $var(\boldsymbol{u}_t) = E(\boldsymbol{u}_t\boldsymbol{u}_t') = \boldsymbol{\Sigma} = \boldsymbol{A}_0^{-1}(\boldsymbol{A}_0^{-1})'$ is the $n \times n$ variance-covariance matrix of reduced-form errors. Let $\boldsymbol{\phi} = (\boldsymbol{B}, \boldsymbol{\Sigma}) \in \boldsymbol{\Phi}$ collect the reduced-form parameters, where $\boldsymbol{B} \equiv [\boldsymbol{b}, \boldsymbol{B}_1, \ldots, \boldsymbol{B}_p]$, $\boldsymbol{\Phi} \subset \mathcal{R}^{n+n^p} \times \boldsymbol{\Xi}$, and $\boldsymbol{\Xi}$ is the space of symmetric positive semidefinite matrices. Note that $\boldsymbol{\Phi}$ is such that the VAR(p) is invertible into a VMA(∞), i.e., the model is stationary. Thus, the VMA(∞) representation of (2.2) is

$$\boldsymbol{y}_t = \boldsymbol{c} + \sum_{j=0}^{\infty} \boldsymbol{C}_j(\boldsymbol{B})\boldsymbol{A}_0^{-1}\boldsymbol{\epsilon}_{t-j}, \tag{2.3}$$

where $\boldsymbol{C}_j(\boldsymbol{B})$ is the j-th coefficient matrix of $(\boldsymbol{I}_n - \sum_{j=1}^{p} \boldsymbol{B}_j L^j)^{-1}$. Let the $n \times n$ matrix

$$\boldsymbol{IR}^h = \boldsymbol{C}_h(\boldsymbol{B})\boldsymbol{A}_0^{-1} \tag{2.4}$$

be the impulse response at h-th horizon for $h = 0, 1, \ldots,$ where its (i, j)-element denotes the effect on the i-th variable in $\boldsymbol{y}_{t+h}$ of a unit shock to the j-th element of $\boldsymbol{\epsilon}_t$.

2.2 The Identification Problem

In absence of any identifying restrictions, Uhlig (2005) shows that $\{\boldsymbol{A}_0 = \boldsymbol{Q}'\boldsymbol{\Sigma}_{tr}^{-1} : \boldsymbol{Q} \in \boldsymbol{\Theta}(n)\}$ is the set of observationally equivalent $\boldsymbol{A}_0$'s consistent with reduced-form parameters, where $\boldsymbol{\Sigma}$ relates to $\boldsymbol{A}_0$ by $\boldsymbol{\Sigma} = \boldsymbol{A}_0^{-1}(\boldsymbol{A}_0^{-1})'$, $\boldsymbol{\Sigma}_{tr}$ denotes the lower triangular Cholesky matrix with non-negative diagonal coefficients and $\boldsymbol{Q} \in \boldsymbol{\Theta}(n)$, known as rotation matrix, is the $n \times n$ orthonormal matrix belonging to the space of $n \times n$ orthonormal matrices $\boldsymbol{\Theta}(n)$. The likelihood function depends on $\boldsymbol{\phi}$ and does not contain any information about $\boldsymbol{Q}$, leading to ambiguity in decomposing $\boldsymbol{\Sigma}$. Thus, there is a multiplicity of $\boldsymbol{Q}$'s which deliver $\boldsymbol{A}_0$ given $\boldsymbol{\phi}$. Similarly, the rest of structural parameters $\boldsymbol{A}_+$ is a function of $\boldsymbol{Q}$ and Cholesky decomposition of reduced-form parameters. For simplicity, this Section illustrates the identification problem relying on $\boldsymbol{A}_0$ only.

This paper focuses on set-identification, so there will be fewer than $n-j$ equality restrictions on the j-th structural shock;[3] thus, no matter how many sign restrictions are imposed, point-identification fails and there will only be set-identification. I follow Christiano, Eichenbaum, and Evans (1999) and assume that the diagonal elements of $\boldsymbol{A}_0$ are non-negative, i.e., a structural shock is a one standard-deviation positive shock to the related variable. As a result, the set of observationally equivalent $\boldsymbol{A}_0$'s becomes $\{\boldsymbol{A}_0 = \boldsymbol{Q}'\boldsymbol{\Sigma}_{tr}^{-1} : \boldsymbol{Q} \in \boldsymbol{\Theta}(n), diag(\boldsymbol{Q}'\boldsymbol{\Sigma}_{tr}^{-1}) \geq \boldsymbol{0}\}$, where $diag(\bullet) \geq \boldsymbol{0}$ implies that all diagonal elements of $\bullet$ are non-negative. Thus, in absence of any identifying restrictions, there is a multiplicity of $\boldsymbol{Q}$'s consistent with $\boldsymbol{A}_0$, given the reduced-form parameters:

$$\boldsymbol{\mathcal{Q}}(\boldsymbol{\phi}) = \{\boldsymbol{Q} \in \boldsymbol{\Theta}(n) : diag(\boldsymbol{Q}'\boldsymbol{\Sigma}_{tr}^{-1}) \geq \boldsymbol{0}\}.$$

Without loss of generality, suppose one is interested in a specific (structural) impulse response - for instance, the $(i,j)-$th element of $\boldsymbol{IR}^h$ -:

$$g_{ij}^h(\boldsymbol{\phi}, \boldsymbol{Q}) \equiv \boldsymbol{e}_i'\boldsymbol{C}_h(\boldsymbol{B})\boldsymbol{\Sigma}_{tr}\boldsymbol{Q}\boldsymbol{e}_j \equiv \boldsymbol{c}_{ih}'(\boldsymbol{\phi})\boldsymbol{q}_j,$$

where $g_{ij}^h(\boldsymbol{\phi}, \boldsymbol{Q}) \in \mathcal{R}$, $\boldsymbol{e}_i$ is the i-th column vector of $\boldsymbol{I}_n$, $\boldsymbol{q}_j$ is the j-th column of $\boldsymbol{Q}$ and $\boldsymbol{c}_{ih}'(\boldsymbol{\phi})$ represents the i-th row vector of $\boldsymbol{C}_h(\boldsymbol{B})\boldsymbol{\Sigma}_{tr}$. Note that the analysis for the impulse responses can be easily extended to the structural parameters $\boldsymbol{A}_0$ and $\boldsymbol{A}_+$ since each structural parameter can be expressed by the inner product of a vector depending on $\boldsymbol{\phi}$ and a column vector of $\boldsymbol{Q}$.

2.2.1 Equality Restrictions

Typical equality restrictions include zero restrictions on off-diagonal elements of $\boldsymbol{A}_0^{-1}$, which correspond to a subset of the restrictions imposed by the classical recursive identification scheme that sets the upper-triangular elements of $\boldsymbol{A}_0^{-1}$ to zero. The econometric framework here also allows to place zero restrictions on the lagged coefficients $\boldsymbol{A}_l : l = 1, \dots p$ and restrictions on the long-run impulse responses $\boldsymbol{IR}^\infty = (\boldsymbol{I}_n - \sum_{j=1}^p \boldsymbol{B}_j)^{-1}\boldsymbol{\Sigma}_{tr}\boldsymbol{Q}$. For simplicity and without loss of generality, this paper reduces the set of equality restrictions to zero restrictions only (in the short- or in the long-run). They can be considered as linear constraints on the columns of $\boldsymbol{Q}$ with coefficients depending on the reduced-form parameters $\boldsymbol{\phi}$. As a result, zero restrictions

[3] The set of $\boldsymbol{A}_0$ and $\boldsymbol{A}_+$ collapses to a singleton as long as identifying assumptions are able to deliver a unique $\boldsymbol{Q}$ which recovers structural parameter $\boldsymbol{A}_0$ and $\boldsymbol{A}_+$, i.e. point-identification. Rothenberg (1971) proves that necessary condition for point-identification require that the number of equality restrictions is greater than or equal to $n(n-1)/2$. Rubio-Ramirez, Waggoner, and Zha (2010) establish sufficient conditions for point-identification: there must be at least $n-j$ equality restrictions on the j-th structural shock, for $1 \leq j \leq n$, and sign normalizations on the impulse responses to each structural shock.

can be represented as follows:

$$\boldsymbol{F}(\boldsymbol{\phi},\boldsymbol{Q}) \equiv \begin{pmatrix} \boldsymbol{F}_1(\boldsymbol{\phi})\boldsymbol{q}_1 \\ \vdots \\ \boldsymbol{F}_n(\boldsymbol{\phi})\boldsymbol{q}_n \end{pmatrix} = \mathbf{0}, \quad \boldsymbol{F}_i(\phi)\colon\ f_i \times n, \tag{2.5}$$

where $f_i \times n$ matrix $\boldsymbol{F}_i(\boldsymbol{\phi})$ depends on $\boldsymbol{\phi}$. Each row vector in $\boldsymbol{F}_i(\boldsymbol{\phi})$ is the coefficient vector of a zero restriction that constrains the correspondent column of $\boldsymbol{Q}$. More generally, $\boldsymbol{F}_i(\boldsymbol{\phi})$ collects all the coefficient vectors that multiply $\boldsymbol{q}_i$ into a matrix and f_i denotes number of zero restrictions constraining $\boldsymbol{q}_i$.

2.2.2 Sign Restrictions

Assume that the researcher is interested in imposing some sign restrictions on the impulse response vector to the j-th structural shock and let s_{hj} denote the number of sign restrictions on impulse responses at horizon h. In this case, the impulse response is given by the j-th column vector of $\boldsymbol{IR}^h = \boldsymbol{C}_h(\boldsymbol{B})\boldsymbol{\Sigma}_{tr}\boldsymbol{Q}$ and the sign restrictions are

$$\boldsymbol{S}_{hj}(\boldsymbol{\phi})\boldsymbol{q}_j \geq \mathbf{0},$$

where $\boldsymbol{S}_{hj}(\boldsymbol{\phi}) \equiv \boldsymbol{D}_{hj}\boldsymbol{C}_h(\boldsymbol{B})\boldsymbol{\Sigma}_{tr}$ is a $s_{hj} \times n$ matrix and $\boldsymbol{D}_{hj}$ is the $s_{hj} \times n$ selection matrix that selects the sign-restricted responses from the $n \times 1$ response vector $\boldsymbol{C}_h(\boldsymbol{B})\boldsymbol{\Sigma}_{tr}\boldsymbol{q}_j$. The nonzero elements of $\boldsymbol{D}_{hj}$ can be equal to 1 or to -1 depending on the sign of restriction on the impulse response of interest. By considering multiple horizons, the whole set of sign restrictions placed on the $j-$th shock is

$$\boldsymbol{S}_j(\boldsymbol{\phi})\boldsymbol{q}_j \geq \mathbf{0}. \tag{2.6}$$

Specifically, $\boldsymbol{S}_j$ is a $\left(\sum_{h=0}^{\bar{h}_j} s_{hj}\right) \times n$ matrix defined by $\boldsymbol{S}_j(\boldsymbol{\phi}) = \left[\boldsymbol{S}'_{0j}(\boldsymbol{\phi}), \ldots, \boldsymbol{S}'_{\bar{h}_j j}(\boldsymbol{\phi})\right]'$. Let $\mathcal{I}_{\mathcal{S}} \subset \{1, 2, \ldots, n\}$ be the set of indices such that $j \in \mathcal{I}_{\mathcal{S}}$ if some of the impulse responses to the j-th structural shock are sign-constrained. Thus, the set of all sign restrictions is

$$\boldsymbol{S}_j(\boldsymbol{\phi})\boldsymbol{q}_j \geq \mathbf{0}, \text{ for } j \in \mathcal{I}_{\mathcal{S}}. \tag{2.7}$$

With abuse of notation, let $\boldsymbol{S}(\boldsymbol{\phi},\boldsymbol{Q}) \geq 0$ collect all sign restrictions $\boldsymbol{S}_j(\boldsymbol{\phi})\boldsymbol{q}_j \geq 0$ for any $j \in \mathcal{I}_{\mathcal{S}}$.[4]

[4] Given the j-th shock, sign restrictions on $\boldsymbol{A}_0$ and $\boldsymbol{A}_+$ can be appended to equation (2.6) as they can be expressed as linear inequalities on $\boldsymbol{q}_j$.

The sign restrictions above can be easily added to the zero restrictions; let $\mathcal{Q}(\phi|F, S)$ be the set of Q's that satisfy sign normalizations, zero and sign restrictions, given ϕ:

$$\mathcal{Q}(\phi|F, S) = \{Q \in \Theta(n) : F(\phi, Q) = \mathbf{0},\ S(\phi, Q) \geq \mathbf{0},\ diag(Q'\Sigma_{tr}^{-1}) \geq \mathbf{0}\}.$$

The identified set for the object of interest is a set-valued map from ϕ to a subset in $\mathcal{R}$ that delivers the range of $g_{ij}^{h}(\phi, Q)$ when Q varies over $\mathcal{Q}(Q|F, S)$:

$$IS_g(\phi|F, S) = \{g_{ij}^{h}(\phi, Q) : Q \in \mathcal{Q}(\phi|F, S)\}. \tag{2.8}$$

3 Bounds on the Forecast Error Variance Decomposition

While zero and sign restrictions are well-established tools to identify shocks, this Section introduces constraints on the bounds of the FEVD. First, it explains how bounds on the FEVD shape the identified set. Second, it analytically illustrates the reduction in the identified set implied by bounds on the FEVD in static bivariate and trivariate models; interestingly, the identified set gets smaller also for structural objects which are not subject to the restrictions. Third, for higher-dimensional SVARs it provides conditions for non-emptiness and reduction. Fourth, it presents a robust-prior procedure for estimation and inference.

3.1 The Forecast Error Variance

The $\tilde{h}$-step ahead Forecast Error (FE) for a SVAR as in equation (2.1), given all the data up to $t-1$, is $FE(\tilde{h}) \equiv y_{t+\tilde{h}} - y_{t+\tilde{h}|t-1} = \sum_{h=0}^{\tilde{h}} IR^{h}\epsilon_{t+\tilde{h}-h}$. Thus, the FEV at horizon $\tilde{h}$ is

$$FEV(\tilde{h}) \equiv E\left[(y_{t+\tilde{h}} - y_{t+\tilde{h}|t-1})(y_{t+\tilde{h}} - y_{t+\tilde{h}|t-1})'\right] = \sum_{h=0}^{\tilde{h}} IR^{h} IR^{h\prime}.$$

As a result, the contribution of shock j to the FEV of variable z at horizon $\tilde{h}$ is

$$CFEV_j^z(\tilde{h}) \equiv \frac{FEV_j^z(\tilde{h})}{FEV^z(\tilde{h})} = \frac{\sum_{h=0}^{\tilde{h}} IR_{z,j}^{h2}}{\sum_{j=1}^{n}\sum_{h=0}^{\tilde{h}} IR_{z,j}^{h2}}, \tag{3.1}$$

where $FEV_j^z(\tilde{h}) = \sum_{h=0}^{\tilde{h}} IR_{z,j}^{h2}$ is the FEV of variable z due to shock j at horizon $\tilde{h}$, $FEV^z(\tilde{h}) = \sum_{j=1}^{n}\sum_{h=0}^{\tilde{h}} IR_{z,j}^{h2}$ denotes the total FEV of variable z at horizon $\tilde{h}$, $IR_{z,j}^{h}$ represents the (z, j)-th element of IR^{h}, and $0 \leq CFEV_j^z(\tilde{h}) \leq 1$. Uhlig (2004b) shows that equation (3.1) can be written as

$$CFEV_j^z(\tilde{h}) = q_j' \Upsilon^z(\phi) q_j, \tag{3.2}$$

where $\boldsymbol{\Upsilon}^z(\boldsymbol{\phi}) = \frac{\sum_{h=0}^{\tilde{h}} \boldsymbol{c}_{zh}(\boldsymbol{\phi})\boldsymbol{c}'_{zh}(\boldsymbol{\phi})}{\sum_{h=0}^{\tilde{h}} \boldsymbol{c}'_{zh}(\boldsymbol{\phi})\boldsymbol{c}_{zh}(\boldsymbol{\phi})}$ is a positive semidefinite $n \times n$ real matrix. Note that $\boldsymbol{\Upsilon}^z(\boldsymbol{\phi})$ also depends on $\tilde{h}$; in order to avoid heavy notation, $\tilde{h}$ is omitted.

Suppose that researcher believes the contribution of shock j to FEV of variable z at horizon $\tilde{h}$ is bounded between $\underline{k}_j^z$ and $\bar{k}_j^z$, where $0 \leq \underline{k}_j^z \leq \bar{k}_j^z \leq 1$ and for simplicity $\tilde{h}$ is omitted from $\underline{k}_j^z$ and $\bar{k}_j^z$. This implies that

$$\underline{k}_j^z \leq \boldsymbol{q}_j' \boldsymbol{\Upsilon}^z(\boldsymbol{\phi}) \boldsymbol{q}_j \leq \bar{k}_j^z. \tag{3.3}$$

Let $\mathcal{I}_{FEV}$ be a set of of indices such that $j \in I_{FEV}$ if shock j is restricted as in (3.3); let Λ_j be a set of of indices such that $z \in \Lambda_j$, where $j \in \mathcal{I}_{FEV}$, if the FEV of variable $z \in \{1, \ldots, n\}$ to shock j is bounded as in (3.3). Thus, the set of all the bounds on the FEVD can be accordingly expressed by

$$\underline{k}_j^z \leq \boldsymbol{q}_j' \boldsymbol{\Upsilon}^z(\boldsymbol{\phi}) \boldsymbol{q}_j \leq \bar{k}_j^z, \text{ for } j \in \mathcal{I}_{FEV} \text{ and } z \in \Lambda_j. \tag{3.4}$$

As shorthand notation, let $\underline{\boldsymbol{k}} \leq \boldsymbol{\Gamma}(\boldsymbol{\phi}, \boldsymbol{Q}) \leq \bar{\boldsymbol{k}}$ collect the whole set of bounds on the FEVD represented by (3.4). Note that sign restrictions impose linear constraints on the columns of $\boldsymbol{Q}$; on the other hand, bounds on the FEVD place quadratic inequalities.

Thus, the set of $\boldsymbol{Q}$'s that satisfy sign normalizations, zero restrictions, sign restrictions and restrictions on the FEVD is

$$\mathcal{Q}(\boldsymbol{\phi}|\boldsymbol{F}, \boldsymbol{S}, \boldsymbol{\Gamma}) = \{\boldsymbol{Q} \in \boldsymbol{\Theta}(n) : \boldsymbol{F}(\boldsymbol{\phi}, \boldsymbol{Q}) = \boldsymbol{0},\ \boldsymbol{S}(\boldsymbol{\phi}, \boldsymbol{Q}) \geq \boldsymbol{0},\ \underline{\boldsymbol{k}} \leq \boldsymbol{\Gamma}(\boldsymbol{\phi}, \boldsymbol{Q}) \leq \bar{\boldsymbol{k}},\ diag(\boldsymbol{Q}'\boldsymbol{\Sigma}_{tr}^{-1}) \geq \boldsymbol{0}\}.$$

The correspondent identified set for the object of interest is:

$$IS_g(\boldsymbol{\phi}|\boldsymbol{F}, \boldsymbol{S}, \boldsymbol{\Gamma}) = \{g_{ij}^h(\boldsymbol{\phi}, \boldsymbol{Q}) : \boldsymbol{Q} \in \mathcal{Q}(\boldsymbol{\phi}|\boldsymbol{F}, \boldsymbol{S}, \boldsymbol{\Gamma})\}. \tag{3.5}$$

Note that the identified set induced by inequality constraints on the FEVD and/or sign restrictions can be empty, as opposed to the case with zero restrictions only. Section 6.3 establishes conditions to deliver non-empty sets.

3.2 Small-Scale framework

This Section analytically illustrates the reduction in the identified set implied by bounds on the FEVD in static bivariate and trivariate models; interestingly, the identified set gets smaller also for structural objects which are not subject to the restrictions. Appendix A provides the proofs.

3.2.1 Bivariate Setting

The structural framework is the following:

$$\boldsymbol{A}_0 \begin{pmatrix} y_{1t} \\ y_{2t} \end{pmatrix} = \begin{pmatrix} \epsilon_{1t} \\ \epsilon_{2t} \end{pmatrix}, \quad \boldsymbol{A}_0 = \begin{pmatrix} a_{11} & a_{12} \\ a_{21} & a_{22} \end{pmatrix}, \text{ t=1,...,T}, \tag{3.6}$$

where (y_{1t}, y_{2t}) are two endogenous variables, respectively. $(\epsilon_{1t}, \epsilon_{2t})$ denotes an i.i.d. normally distributed vector of structural shocks with variance-covariance the identity matrix. $\boldsymbol{\theta} = \boldsymbol{A}_0$ collects the structural parameters and the contemporaneous impulse responses are elements of $\boldsymbol{A}_0^{-1}$. The reduced-form model is indexed by $\boldsymbol{\Sigma}$, the variance-covariance matrix of the endogenous variables, which satisfies $\boldsymbol{\Sigma} = \boldsymbol{A}_0^{-1}(\boldsymbol{A}_0^{-1})'$. Let $\boldsymbol{\Sigma}_{tr} = \begin{pmatrix} \sigma_{11} & 0 \\ \sigma_{21} & \sigma_{22} \end{pmatrix}$ denote its lower triangular Cholesky decomposition, where $\sigma_{11} \geq 0$ and $\sigma_{22} \geq 0$. Thus, $\boldsymbol{\phi} = (\sigma_{11}, \sigma_{21}, \sigma_{22}) \in \boldsymbol{\Phi} = \mathbb{R}_+ \times \mathbb{R} \times \mathbb{R}_+$ collects the reduced-form parameters. Following Uhlig (2005), $\boldsymbol{A}_0$ can be parametrized via the Cholesky matrix $\boldsymbol{\Sigma}_{tr}$ and a rotation matrix $\boldsymbol{Q} = \begin{pmatrix} \cos\rho & -\sin\rho \\ \sin\rho & \cos\rho \end{pmatrix}$ with spherical coordinate $\rho \in [0, 2\pi]$. The structural matrix of impact responses can be written as

$$\boldsymbol{IR}^0 = \boldsymbol{A}_0^{-1} = \boldsymbol{\Sigma}_{tr}\boldsymbol{Q} = \begin{pmatrix} \sigma_{11}\cos\rho & -\sigma_{11}\sin\rho \\ \sigma_{21}\cos\rho + \sigma_{22}\sin\rho & -\sigma_{21}\sin\rho + \sigma_{22}\cos\rho \end{pmatrix}.$$

Without loss of generality, let the structural object of interest α be the response of y_1 to a unit shock ϵ_1, $\alpha \equiv \sigma_{11}\cos\rho$.

Two standard sign restrictions (SR) are imposed on IRFs:

- *SR1*

  On impact, positive shock ϵ_2 does not increase variable y_1: $\sigma_{11}\sin\rho \geq 0$. Under this assumption, the conditional covariance induced by ϵ_2 is non-positive.

- *SR2*

  Positive shock ϵ_1 does not reduce variable y_2: $-\sigma_{22}\sin\rho - \sigma_{21}\cos\rho \leq 0$.

Note that standard sign restrictions impose linear inequalities on ρ. Appendix A proves that the identified set for α is

$$IS_\alpha(\boldsymbol{\phi}) \equiv \begin{cases} \left[\sigma_{11}\cos\left(\arctan\left(\frac{\sigma_{22}}{\sigma_{21}}\right)\right), \sigma_{11}\right], & \text{for } \sigma_{21} > 0, \\ \left[0, \sigma_{11}\cos\left(\arctan\left(-\frac{\sigma_{21}}{\sigma_{22}}\right)\right)\right], & \text{for } \sigma_{21} \leq 0. \end{cases} \tag{3.7}$$

- *FEVR*

Assume that the contribution of shock ϵ_2 to the total error variance of y_1 is bounded between $\underline{k}$ and $\bar{k}$; this constrains the FEVD. Following the notation introduced in Section 3, this restriction can be written as $\underline{k} \leq CFEV_{\epsilon_2}^{y_1}(0) \leq \bar{k}$, where $0 \leq \underline{k} < \bar{k} \leq 1$.

SR1, *SR2* and *FEVR* deliver the following identified set for α:

$$IS_\alpha(\boldsymbol{\phi}) \equiv \begin{cases} \left[\sigma_{11}\cos(\arcsin\sqrt{\bar{k}}),\ \sigma_{11}\cos(\arcsin\sqrt{\underline{k}})\right], \\ \text{for } \{\sigma_{21} > 0,\ \bar{k} < \bar{k}^*\} \cup \{\sigma_{21} \leq 0,\ \underline{k} > \underline{k}^*\}, \\ \left[\sigma_{11}\cos\left(\arctan\left(\frac{\sigma_{22}}{\sigma_{21}}\right)\right),\ \sigma_{11}\cos(\arcsin\sqrt{\underline{k}})\right], \\ \text{for } \sigma_{21} > 0,\ \bar{k} \geq \bar{k}^*, \\ \left[\sigma_{11}\cos(\arcsin\sqrt{\bar{k}}),\ \sigma_{11}\cos\left(\arctan\left(-\frac{\sigma_{21}}{\sigma_{22}}\right)\right)\right], \\ \text{for } \sigma_{21} \leq 0,\ \underline{k} \leq \underline{k}^*, \end{cases} \tag{3.8}$$

where $\bar{k}^* = \sin^2\left(\arctan\left(\frac{\sigma_{22}}{\sigma_{21}}\right)\right)$ and $\underline{k}^* = \sin^2\left(\arctan\left(-\frac{\sigma_{21}}{\sigma_{22}}\right)\right)$. The following Proposition formally compares the identified set induced by sign restrictions only with that in (3.8).

Proposition 3.1 *The identified set for the structural impulse response α in (3.8) is strictly smaller than in (3.7) unless $\underline{k} = 0,\ \bar{k} \geq \bar{k}^*,\ \sigma_{21} > 0$ or $\bar{k} = 1,\ \underline{k} \leq \underline{k}^*,\ \sigma_{21} \leq 0$, where the identified sets are equivalent.*

Proposition above provides some interesting insights. First, if both lower and upper bounds are constrained, i.e., $\underline{k} \neq 0,\ \bar{k} \neq 1$, then the restrictions on the FEVD always shrink the identified set of α with respect to the set induced by *SR1* and *SR2* for any $\boldsymbol{\phi} = (\sigma_{11}, \sigma_{21}, \sigma_{22}) \in \boldsymbol{\Phi} = \mathbb{R}_+ \times \mathbb{R} \times \mathbb{R}_+$. Second, suppose that the lower bound is unrestricted; shrinkage then occurs for any $\sigma_{21} \leq 0$ or if $\sigma_{21} > 0$ and $\bar{k} < \bar{k}^*$. In other words, if the lower bound is unrestricted and the unconditional covariance is positive, the upper bound must be low enough to deliver restriction of the identified set. Third, assume that the upper bound is unconstrained; then there is shrinkage for any $\sigma_{21} > 0$ or if $\sigma_{21} \leq 0$ and $\underline{k} > \underline{k}^*$. This implies that if the upper bound is unrestricted and the unconditional covariance is negative, the lower bound must be high enough to deliver restriction of the identified set.

Note that *FEVR* is restricting the FEVD of the variable of interest, namely y_1. However, conditions similar to those in Proposition 3.1 can be easily found for bounds on the FEVD of variables other than y_1.

- *FEVR2*

  Suppose that the contribution of shock ϵ_1 to the total error variance of y_2 is bounded as follows: $\underline{k} \leq CFEV_{\epsilon_1}^{y_2}(0) \leq \bar{k}$, where $0 \leq \underline{k} < \bar{k} \leq 1$.

Appendix A provides the details of the following proposition, in which $\bar{k}^{**}$ and $\underline{k}^{**}$ denote functions of reduced-form parameters.

Proposition 3.2 *The identified set for the structural impulse response α induced by SR1, SR2 and FEVR2 is strictly smaller than in (3.7) unless $\underline{k} = 0,\ \bar{k} \geq \bar{k}^{**},\ \sigma_{21} \leq 0$ or $\bar{k} = 1,\ \underline{k} \leq \underline{k}^{**},\ \sigma_{21} > 0$, where the identified sets are equivalent.*

3.2.2 Trivariate Setting

The bivariate illustration shows that bounds on the FEVD shrink the set induced by sign restrictions. Higher dimensional cases are more complex. However, while Proposition 3.1 and 3.2 are easily replicable in a trivariate framework, this is useful to show the effect of bounds on the FEVD of variables and shocks other than those in the object of interest.

The structural framework is the following:

$$\boldsymbol{A}_0 \begin{pmatrix} y_{1t} \\ y_{2t} \\ y_{3t} \end{pmatrix} = \begin{pmatrix} \epsilon_{1t} \\ \epsilon_{2t} \\ \epsilon_{3t} \end{pmatrix}. \tag{3.9}$$

The reduced-form model is indexed by $\boldsymbol{\Sigma}$, the variance-covariance matrix of the endogenous variables, which satisfies $\boldsymbol{\Sigma} = \boldsymbol{A}_0^{-1}(\boldsymbol{A}_0^{-1})'$. Let $\boldsymbol{\Sigma}_{tr} = \begin{pmatrix} \sigma_{11} & 0 & 0 \\ \sigma_{21} & \sigma_{22} & 0 \\ \sigma_{31} & \sigma_{32} & \sigma_{33} \end{pmatrix}$ denote its lower triangular Cholesky decomposition, where $\sigma_{11} \geq 0$, $\sigma_{22} \geq 0$ and $\sigma_{33} \geq 0$. $\boldsymbol{\phi} = (\sigma_{11}, \sigma_{21}, \sigma_{22}, \sigma_{31}, \sigma_{32}, \sigma_{33})$ collects the reduced-form parameters. Let the structural object of interest α be the response of y_1 to a unit positive shock ϵ_1, $\alpha \equiv \sigma_{11}\cos\rho$, where $\rho \in [0, 2\pi]$.

Three standard sign restrictions (SR) are imposed.

- *SR1*

  On impact, positive shock ϵ_3 does not increase variable y_1: $\sigma_{11}\sin\rho \geq 0$.

- *SR2*

  Positive shock ϵ_1 does not reduce variable y_2 on impact: $\sigma_{21}\cos\rho \geq 0$.

- *SR3*

  Positive shock ϵ_1 does not decrease variable y_3 on impact: $\sigma_{31}\cos\rho + \sigma_{33}\sin\rho \geq 0$.

The implied identified set for α is

$$IS_\alpha(\boldsymbol{\phi}) \equiv \begin{cases} \left[\sigma_{11}\cos\left(\arctan\left(\frac{\sigma_{33}}{\sigma_{31}}\right)\right),\ \sigma_{11}\right], & \text{for } \sigma_{31} > 0, \\ \left[0,\ \sigma_{11}\cos\left(\arctan\left(-\frac{\sigma_{31}}{\sigma_{33}}\right)\right)\right], & \text{for } \sigma_{31} \leq 0, \end{cases} \tag{3.10}$$

where sign restrictions are defined only over $\sigma_{21} \geq 0$.

- *FEVR3*

  Suppose that the contribution of shock ϵ_3 to the total error variance of y_2 is bounded as follows: $\underline{k} \leq CFEV_{\epsilon_3}^{y_2}(0) \leq \bar{k}$, where $0 \leq \underline{k} < \bar{k} \leq 1$.

The identified set induced by *SR1*, *SR2*, *SR3*, and *FEVR3* is

$$IS_\alpha(\boldsymbol{\phi}) \equiv \begin{cases} \left[\sigma_{11}\cos\left(\arcsin\left(\frac{\sqrt{\bar{k}(\sigma_{21}^2+\sigma_{22}^2)}}{\sigma_{21}}\right)\right),\ \sigma_{11}\cos\left(\arcsin\left(\frac{\sqrt{\underline{k}(\sigma_{21}^2+\sigma_{22}^2)}}{\sigma_{21}}\right)\right)\right], \\ \text{for } \{\sigma_{31} > 0,\ \bar{k} < \bar{k}^*\} \cup \{\sigma_{31} \leq 0,\ \underline{k} > \underline{k}^*\}, \\ \left[\sigma_{11}\cos\left(\arctan\left(\frac{\sigma_{33}}{\sigma_{31}}\right)\right),\ \sigma_{11}\cos\left(\arcsin\left(\frac{\sqrt{\underline{k}(\sigma_{21}^2+\sigma_{22}^2)}}{\sigma_{21}}\right)\right)\right], \\ \text{for } \sigma_{31} > 0,\ \bar{k} \geq \bar{k}^*, \\ \left[\sigma_{11}\cos\left(\arcsin\left(\frac{\sqrt{\bar{k}(\sigma_{21}^2+\sigma_{22}^2)}}{\sigma_{21}}\right)\right),\ \sigma_{11}\cos\left(\arctan\left(-\frac{\sigma_{31}}{\sigma_{33}}\right)\right)\right], \\ \text{for } \sigma_{31} \leq 0,\ \underline{k} \leq \underline{k}^*, \end{cases} \tag{3.11}$$

where $\underline{k}^* = \frac{\sigma_{21}^2}{\sigma_{21}^2+\sigma_{22}^2}\sin^2\left(\arctan\left(-\frac{\sigma_{31}}{\sigma_{33}}\right)\right)$, $\bar{k}^* = \frac{\sigma_{21}^2}{\sigma_{21}^2+\sigma_{22}^2}\sin^2\left(\arctan\left(\frac{\sigma_{33}}{\sigma_{31}}\right)\right)$, and $\sigma_{21} \geq 0$. Comparison between (3.10) and (3.11) leads to the following proposition.

Proposition 3.3 *The identified set for the structural impulse response α in (3.11) is strictly smaller than in (3.10) unless $\underline{k} = 0,\ \bar{k} \geq \bar{k}^*,\ \sigma_{31} > 0$ or $\bar{k} = 1,\ \underline{k} \leq \underline{k}^*,\ \sigma_{31} \leq 0$, where the identified sets are equivalent.*

3.3 Non-Emptiness and Reduction of the Identified Set

The previous Section showed that bounds on the FEVD reduce the identified set for small-scale models. However, there is a well-known trade-off between sharp identification and computation (Uhlig, 2017; Amir-Ahmadi and Drautzburg, 2018; Giacomini and Kitagawa, 2018; Gafarov, Meier, and Olea, 2018). In fact, tight restrictions could potentially lead to sets with zero measure, or empty sets; thus, it is crucial to distinguish when the identification is sharp because the identified set has a reduced, but positive, measure and when constraints are too tight and lead to empty sets. Thus, this Section addresses this trade-off and (i) provides sufficient conditions for assessing whether constraints on the FEVD deliver a non-empty set, (ii) establishes necessary conditions for reduction of the set under bounds on the FEVD for any-scale SVARs, where closed-form characterization of the identified set is hard.

For the results in this Section, it is useful to introduce some more notation. Let $\boldsymbol{\Upsilon}^z_S(\boldsymbol{\phi}) = \frac{\boldsymbol{\Upsilon}^z(\boldsymbol{\phi})+(\boldsymbol{\Upsilon}^z(\boldsymbol{\phi}))'}{2}$ denote the symmetric part of $\boldsymbol{\Upsilon}^z(\boldsymbol{\phi})$, where $z \in \Lambda_j$; $\lambda^z_{l,j}$ for $l = \{1, \dots, n\}$ are the n real eigenvalues of $\boldsymbol{\Upsilon}^z_S(\boldsymbol{\phi})$. Note that $\lambda^z_{max,j} = max\{\lambda^z_{1,j}, \dots, \lambda^z_{n,j}\}$ and $\lambda^z_{min,j} = min\{\lambda^z_{1,j}, \dots, \lambda^z_{n,j}\}$. Finally, let $\tilde{\boldsymbol{q}}$ be the eigenvector associated to $\lambda^z_{l,j}$, namely $\boldsymbol{\Upsilon}^z_S(\boldsymbol{\phi})\tilde{\boldsymbol{q}} = \lambda^z_{l,j}\tilde{\boldsymbol{q}}$.

Proposition 3.4 establishes conditions for non-emptiness of $IS_g(\boldsymbol{\phi}|\boldsymbol{F}, \boldsymbol{S}, \boldsymbol{\Gamma})$.

Proposition 3.4 *(Non-emptiness) Let* $\{g^h_{ij^*}(\boldsymbol{\phi}, \boldsymbol{Q}) = \boldsymbol{c}'_{ih}(\boldsymbol{\phi})\boldsymbol{q}_{j^*} : i = 1, \dots, n, h = 0, 1, \dots\}$ *denote the impulse responses to the* j^*-th *shock. Assume that identifying restrictions are placed on the* j^*-th *structural shock only, i.e.,* $f_i = 0 \ for \ i \neq j^*$, $\mathcal{I_S} = \mathcal{I_{FEV}} = \{j^*\}$ *and let* $z, z^* \in \{1, \dots, n\}$. *If the following conditions hold*

(a) $\exists z \in \Lambda_{j^*} \mid \underline{k}^z_{j^*} \leq \lambda^z_{l,j^*} \leq \bar{k}^z_{j^*},\ \boldsymbol{\Upsilon}^z_S(\boldsymbol{\phi})\tilde{\boldsymbol{q}} = \lambda^z_{l,j^*}\tilde{\boldsymbol{q}}$ *for some* $l = \{1, \dots, n\}$,

(b) $\underline{k}^{z^*}_{j^*} \leq \tilde{\boldsymbol{q}}'\boldsymbol{\Upsilon}^{z^*}(\boldsymbol{\phi})\tilde{\boldsymbol{q}} \leq \bar{k}^{z^*}_{j^*}\ \forall z^* \neq z \in \Lambda_{j^*},\ \boldsymbol{S}_{j^*}(\boldsymbol{\phi})\tilde{\boldsymbol{q}} \geq \boldsymbol{0},\ \boldsymbol{F}_{j^*}(\boldsymbol{\phi})\tilde{\boldsymbol{q}} = \boldsymbol{0}$,

then the identified set $IS_g(\boldsymbol{\phi}|\boldsymbol{F}, \boldsymbol{S}, \boldsymbol{\Gamma})$ *is non-empty and bounded.*

The main assumption is that restrictions constrain a single shock; however, in the empirical literature this is relatively common (Uhlig, 2005; Dedola and Neri, 2007; Vargas-Silva, 2008; Scholl and Uhlig, 2008; Rafiq and Mallick, 2008; Fujita, 2011; Dedola, Rivolta, and Stracca, 2017). If there is a $z \in \Lambda_{j^*}$ satisfying condition (a), constraint $\underline{k}^z_{j^*} \leq \boldsymbol{q}'_{j^*}\boldsymbol{\Upsilon}^z(\boldsymbol{\phi})\boldsymbol{q}_{j^*} \leq \bar{k}^z_{j^*}$ is fulfilled for $\boldsymbol{q}_{j^*} = \tilde{\boldsymbol{q}}$, where $\tilde{\boldsymbol{q}}$ is the eigenvector associated to λ^z_{l,j^*} and, as such, is analytically available. If $\tilde{\boldsymbol{q}}$ satisfies remaining restrictions (condition b), the set is then non-empty. If one wanted to verify whether a specific restriction on the FEVD induces a non-empty set, she/he would need to apply conditions (a) and (b) to that constraint.

The following Algorithm implements Proposition 3.4.

Algorithm 3.1

Step 1: Draw $\boldsymbol{\phi}$ *from posterior distribution of the reduced-form VAR.*

Step 2: Select $z \in \Lambda_{j^*}$ *and compute the correspondent eigenvalues* λ^z_{l,j^*} *of* $\boldsymbol{\Upsilon}^z_S(\boldsymbol{\phi})$ *for* $l = \{1, \dots, n\}$.

Step 3: Store $\forall\lambda^z_{l,j^*} \mid \underline{k}^z_{j^*} \leq \lambda^z_{l,j^*} \leq \bar{k}^z_{j^*}$; *otherwise, i.e.,* $\nexists\lambda^z_{l,j^*} \mid \underline{k}^z_{j^*} \leq \lambda^z_{l,j^*} \leq \bar{k}^z_{j^{l}*}$, $IS_g(\boldsymbol{\phi}|\boldsymbol{F}, \boldsymbol{S}, \boldsymbol{\Gamma})$ *is empty.*

Step 4: If $\exists\lambda^z_{l,j^*}$ *such that the associated eigenvector* $\tilde{\boldsymbol{q}}$ *satisfies the remaining restrictions, then* $IS_g(\boldsymbol{\phi}|\boldsymbol{F}, \boldsymbol{S}, \boldsymbol{\Gamma})$ *is non-empty. Otherwise, go back to Step 2 and select* $z^* \neq z \in \Lambda_{j^*}$.

Proposition 3.4 is potentially characterised by a grey area, where sufficient conditions do not hold. However, in the empirical application sufficient conditions are satisfied in more than

75% of the draws. If these conditions fail, the paper sticks to the common literature and the identified set it empty if, for a number of draws from the orthonormal space, an admissible rotation matrix $\boldsymbol{Q}$ cannot be found.

Proposition 3.5 builds on the non-emptiness to derive necessary conditions for reduction of the identified set; this is useful when analytical characterization of the identified set, eg the 2- and 3-variable model in Section 3.2, is not feasible.

Proposition 3.5 *(Shrinkage) Let* $\{g^h_{ij^*}(\boldsymbol{\phi}, \boldsymbol{Q}) = \boldsymbol{c}'_{ih}(\boldsymbol{\phi})\boldsymbol{q}_{j^*} : i = 1, \ldots, n, h = 0, 1, \ldots\}$ *denote the impulse responses to the* j^*-th *shock. Assume that Proposition 3.4 holds and let* $z \in \{1, \ldots, n\}$*. If* $IS_g(\boldsymbol{\phi}|\boldsymbol{F}, \boldsymbol{S}, \boldsymbol{\Gamma}) \subset IS_g(\boldsymbol{\phi}|\boldsymbol{F}, \boldsymbol{S})$*, then* $\exists z \in \Lambda_{j^*} \mid \lambda^z_{min,j^*} < \underline{k}^z_{j^*}$ *or* $\lambda^z_{max,j^*} > \bar{k}^z_{j^*}$*.*

Note that conditions for reduction regard the eigenvalues of $\boldsymbol{\Upsilon}^z_S(\boldsymbol{\phi})$, which only depends on the reduced-form, and as such, are easy-to-check.

3.4 Estimation and Inference

For set-identified SVARs, estimation and inference is not straightforward. The posterior distribution of structural parameters and IRFs reflects uncertainty about the reduced-form parameters $\boldsymbol{\phi}$ and the rotation matrix $\boldsymbol{Q}$. The common approach is to impose a uniform distribution on $\boldsymbol{Q}$ in the space of orthonormal matrices. However, Baumeister and Hamilton (2015) show that this choice does not imply a uniform distribution over the identified set of the structural parameters, because the latter are a function of reduced-form parameters and rotation matrix. Additionally, since $\boldsymbol{Q}$ cannot get updated by data, as opposed to reduced-form parameters, Baumeister and Hamilton (2015) stress that, even asymptotically, the posterior of structural parameters is proportional to the prior distribution. Furthermore, Arias, Rubio-Ramirez, and Waggoner (2017) point out that practicioners are likely to combine sign and zero restrictions by introducing unintended prior information.

The paper addresses the criticism by Baumeister and Hamilton (2015) and Arias, Rubio-Ramirez, and Waggoner (2017) by computing, under a convexity criterion, the infimum and supremum over all admissible rotation matrices. This implies that the identified set is distribution-free, i.e., it does not depend on a specific prior over $\boldsymbol{Q}$. Specifically, the set is conditional on reduced-form parameters $\boldsymbol{\phi}$ and, as such, reflects the reduced-form parameter uncertainty. For sign and zero restrictions only, a similar solution has been proposed by Giacomini and Kitagawa (2018), Gafarov, Meier, and Olea (2018), and Amir-Ahmadi and Drautzburg (2018); this paper suggests a distribution-free identified set subject to bounds on the FEVD. As common in literature (Giacomini and Kitagawa, 2018; Gafarov, Meier, and Olea, 2018), characterization of the set is defined for models that place restrictions on a single shock.[5] Furthermore, since the convexity criterion is greatly simplified without zero restrictions, for simplicity the baseline procedure in Algorithm 3.2 excludes equality constraints; details on how to incorporate zero restrictions are provided at the end of this Section.

Specifically, Algorithm 3.2 describes the steps for estimation of the identified set of $g^h_{ij^*}(\boldsymbol{\phi}, \boldsymbol{Q}) = \boldsymbol{c}'_{ih}(\boldsymbol{\phi})\boldsymbol{q}_{j^*}$ for some $i = \{1, \dots, n\}$, $h = 0, 1, \dots,$ and a shock of interest $j^* \in \{1, \dots, n\}$.

Algorithm 3.2

Step 1: Draw $\boldsymbol{\phi}$ from posterior distribution of the reduced-form VAR.

Step 2: If $IS_g(\boldsymbol{\phi}|\boldsymbol{S}, \boldsymbol{\Gamma})$ is non-empty, go to Step 3. Otherwise, go back to Step 1.

Step 3: Compute the bounds of the object of interest:

$$\min_{q_{j^*}} \text{ and } \max_{q_{j^*}} \boldsymbol{c}'_{ih}(\boldsymbol{\phi})\boldsymbol{q}_{j^*}$$
$$s.t.\ \boldsymbol{S}_{j^*}(\boldsymbol{\phi})\boldsymbol{q}_{j^*} \geq \boldsymbol{0},\ \underline{k}^z_{j^*} \leq \boldsymbol{q}'_{j^*}\boldsymbol{\Upsilon}^z(\boldsymbol{\phi})\boldsymbol{q}_{j^*} \leq \bar{k}^z_{j^*} \text{ for any } z \in \Lambda_{j^*},\ ||\boldsymbol{q}_{j^*}|| = 1.$$

Step 4: Repeat Step 1-3 L times.[6]

In the language of Giacomini and Kitagawa (2018) and Amir-Ahmadi and Drautzburg (2018), Algorithm 3.2 delivers prior-robust estimation and inference because it is not dependent on a specific prior over the identified set. Thus, according to DiTraglia and García-Jimeno (2016), it is also frequentist friendly and fully complies with the principle of transparent parametrization invoked by Schorfheide (2016). The algorithm relies jointly on a standard sampling from the posterior of reduced form parameters (Step 1), the detection of emptiness (Step 2) and a numerical optimization to derive bounds (Step 3), i.e., solving a constrained optimization problem. The latter consists in a linear objective function with linear inequality, quadratic inequality and equality constraints. Put it another way, for medium- and high-scale models, Algorithm 3.2 mirrors the analytical characterization of the identified set in the 2- and 3-variable framework in Section 3.2. In order to work, numerical optimization in Step 3 needs to be convex. As a result, following Proposition establishes convexity conditions:

Proposition 3.6 *(Convexity) Let $\{g^h_{ij^*}(\boldsymbol{\phi}, \boldsymbol{Q}) = \boldsymbol{c}'_{ih}(\boldsymbol{\phi})\boldsymbol{q}_{j^*} : i = 1, \dots, n, h = 0, 1, \dots\}$ denote the impulse responses to the j^*-th shock. Assume that identifying restrictions are placed on the j^*-th structural shock only, i.e., $\mathcal{I}_{\mathcal{S}} = \mathcal{I}_{\mathcal{FEV}} = \{j^*\}$, there are no zero restrictions, and let $z \in \{1, \dots, n\}$. If one of the following conditions hold*

[5] Amir-Ahmadi and Drautzburg (2018) generalise to multiple shocks at cost of challenging and burdensome practical implementation.

[6] In the empirical application, $L = 10000$.

(a) $\underline{k}^z_{j^*} = 0 \; \forall z \in \Lambda_{j^*}$,

(b) for any $z \in \Lambda_{j^*}$ *subject to bounds on the FEVD up to horizon* $\tilde{h}$*, responses* $g^h_{zj^*}(\boldsymbol{\phi}, \boldsymbol{Q})$ *are sign-restricted for* $h = 0, \ldots, \tilde{h}$*,*

then the identified set $IS_g(\boldsymbol{\phi}|\boldsymbol{S}, \boldsymbol{\Gamma})$ *is convex.*

Appendix A provides the proof. The intuition is that, under condition (a), the space defined by quadratic constraints on $\boldsymbol{q}_{j^*}$ due to the bounds on the FEVD is always convex. On the other hand, condition (b) linearises the restrictions on the FEVD, i.e., it reduces the constraints on the FEVD to linear inequalities on $\boldsymbol{q}_{j^*}$ and, as such, makes the space of admissible rotation matrices convex; in a nutshell, under condition (b) the identifying restrictions are a set of linear inequality constraints on $\boldsymbol{q}_{j^*}$. Thus, this offers great flexibility because distribution-free Algorithms for estimation and inference in Giacomini and Kitagawa (2018), Gafarov, Meier, and Olea (2018), and Amir-Ahmadi and Drautzburg (2018) can be also applied. If Proposition 3.6 fails and the problem is not convex, standard procedure in Arias, Rubio-Ramirez, and Waggoner (2017), which relies on a uniform specification for $\boldsymbol{Q}$, can be used for estimation and inference.

Relative to influential paper by Giacomini and Kitagawa (2018), there are three main differences. First, in order to compute bounds, numerical optimization is used rather than Monte Carlo integration. The latter may be very hard and impractical, especially for medium- and large-size SVARs, and tends to underestimate the bounds. Second, there is an analytical criterion to check for non-emptiness, while Giacomini and Kitagawa (2018) rely on simulation to detect emptiness. Finally, the optimization problem contains quadratic constraints on $\boldsymbol{q}_{j^*}$, i.e., bounds on the FEVD. This is also the main departure from Gafarov, Meier, and Olea (2018), and Amir-Ahmadi and Drautzburg (2018).

In order to include zero restrictions in Step 3 of Algorithm 3.2, convexity criterion in Proposition 3.6 needs to satisfy additional ordering conditions. Specifically, the variables have to be ordered as in Proposition 3 of Giacomini and Kitagawa (2018).

4 How to derive restrictions

The latter Section showed that bounds on the FEVD can help. However, we still need to find a way to choose a reasonable set of constraints. The current Section presents a methodology to derive theory-driven bounds on the FEVD.

To do so, I adapt to the FEVD the approach that Canova and Paustian (2011) use to obtain sign restrictions from DSGE models for the IRFs.[7] The analysis starts from a framework with an approximate state space representation. I investigate the FEVD of the endogenous variables in response to the disturbances for competing parametrizations. In doing so, I assume that all structural parameters are uniformly and independently distributed over sufficiently wide ranges. This allows to establish bounds on the FEVD which are robust to parameter and specification uncertainty. Note that identification restrictions are explicitly inferred and only robust restrictions are admitted. Thus, the methodology depends on generic conditional dynamics and does not rely on a specific parametrization.

4.1 A Benchmark Model with Real and Nominal Frictions

To illustrate the fundamental restrictions a theoretical structure imposes on the FEVD to monetary policy shock, the medium-size New-Keynesian framework is considered. To save on space, this Section introduces the model and Table 1 reports the list of structural parameters and their support; see Appendix C for details about the equilibrium conditions.

The framework contains many shocks and frictions. Specifically, it features sticky nominal price and wage settings that allow for backward inflation indexation, habit formation in consumption and investment adjustment costs that create hump-shaped responses of aggregate demand, and variable capital utilization and fixed costs in production. The stochastic dynamics is driven by seven orthogonal structural shocks. In addition to total factor productivity shocks, the model includes two shocks that affect the intertemporal margin (risk premium shocks and investment-specific technology shocks), two shocks that affect the intratemporal margin (wage and price mark-up shocks), and two policy shocks (exogenous spending and monetary policy shocks). The degree of persistence of shocks includes values most used in literature; see Smets and Wouters (2003) for a discussion about that.

Households maximize a non-separable utility function with consumption of goods and labour effort as arguments over an infinite horizon; $\beta \in [0.985, 0.995]$ is the discount factor. A time-varying external habit variable (λ) appears in the utility function and varies between 0.00 and 0.95, which encompasses most values used and estimated in the literature. Labour is differentiated by a union, leading to some monopoly power over wages and an explicit wage equation, which allows for different degrees of sticky nominal wages (Calvo model). Households rent capital services to firms and establish how much capital to collect subject to the capital adjustment costs. As the capital rental price moves, the utilization of the capital stock can be amended at increasing cost. Firms produce differentiated goods, settle upon labour and capital

[7] Among others, this procedure has been used by Dedola and Neri (2007), Pappa (2009), Peersman and Straub (2009), Lippi and Nobili (2012).

inputs, and set prices (Calvo model). On top of Calvo setting, both prices and wages can be (fully or partially) indexed. Thus, prices are function of current and expected marginal costs, but are also affected by the past inflation rate. The marginal costs depend on wages and the rental rate of capital. Similarly, wages are also determined by past and expected future wages and inflation. The intervals for stickiness and indexation parameters $(\xi_p, \xi_w, \iota_p, \iota_w)$ covers the universe of possible values considered in the literature, including any combination from very flexible, no indexed models to fully sticky, richly indexed models. Given the interest for monetary policy shocks, the equation below reports the log-linearised monetary policy reaction function for the framework considered here:[8]

$$r_t = \rho r_{t-1} + (1-\rho)[r_\pi \pi_t + r_Y(y_t - y_t^p)] + r_{\Delta y}[(y_t - y_t^p) - (y_{t-1} - y_{t-1}^p] + \epsilon_t^r. \quad (4.1)$$

Specifically, the central bank follows a Taylor rule by adjusting the policy interest rate (r_t) to inflation and output gap $(y_t - y_t^p)$, namely the difference between actual and potential output.[9] ρ denotes the degree of interest rate smoothing; $r_{\Delta y}$ captures the effect of short-run variation in the output gap. ϵ_t^r captures the monetary policy shocks and follows an AR(1) process with an IID-Normal error term: $\epsilon_t^r = \rho_r \epsilon_{t-1}^r + \eta_t^r$.[10] As shown in Table 1, the support of parameters of equation (4.1) is large enough to embody most of parametrisations in literature.

4.2 Deducing Robust Restrictions on the FEVD

I draw 10000 structural parameters vectors from uniform distributions in Table 1. For each of them, I compute impulse responses and the correspondent FEVD to a 1 standard deviation positive (contractionary) monetary policy shock for output growth (Δy_t), consumption growth (Δc_t), investment growth (ΔI_t), real wages growth (Δw_t), hours worked (l_y), inflation rate (π_t), and interest rate (i_t). Specifically, 90% intervals are extracted. This trades-off two elements: robustness, which would lead to select large intervals; potential misspecification, under which no restriction will hold with probability one. Table 2 reports the signs of impact impulse responses[11] and the FEVD at horizon $h = 0$. Specifically, $+(-)$ indicate that a certain variable has the 90% probability to response positively (negatively) on impact; ? indicates that the sign of the response cannot be uniquely pinned down; the bounds of the FEVD represent the 5%

[8] See Appendix C for details over the other shocks and equilibrium conditions.

[9] The potential output is the level of output under flexible wages and prices, and without mark-up shocks.

[10] Some authors, e.g., Smets and Wouters (2003) and Smets and Wouters (2005), have proposed to include a permanent monetary policy shock, such as an inflation objective shock. I augmented the model to do so and the role of temporary monetary policy shocks in explaining error variance of the endogenous variables remains unchanged.

[11] These signs are sufficient to disentangle monetary policy shock from other disturbances.

and 95% percentiles. In particular, first row in Table 1 shows that on impact sign of impulses responses to monetary policy shock is uniquely pinned down, with the significant exception of real wages.[12]

Given the large variety of theoretical models embodied, the FEVD in Table 2 shows relatively large intervals; with the notable exception of the interest rates, lower bound is zero for most of variables. However, upper bounds are well-below one for any variables. Broadly speaking, in the short-run monetary policy shock explains the FEV of interest rates more than that of the remaining endogenous variables. While this outcome may be expected in flexible models, where monetary policy has limited impact on real variables also in the short-run, it is also consistent with sticky prices and wages setting, in which demands shocks other than monetary disturbances, such as government spending shocks, investment shocks, and risk premium shocks, have been found to play a dominant role in the short-run business-cycle of real variables.[13] Next Section describes how to use bounds in Table 2 as identifying restrictions and evaluates them through a Monte-Carlo exercise.

5 A Monte-Carlo Experiment

Monte-Carlo experiment in this Section uses the robust information in Table 2 to make a comparison between the performance of identification scheme based on restrictions on the FEVD and sign restrictions. The DGP is the model in Smets and Wouters (2007) calibrated at its posterior means (Table 1A in Smets and Wouters (2007)); the correspondent reduced-form VAR includes the variables listed above and has lag length four. Without loss of generality, I want to evaluate the ability of theory-driven restrictions on the FEVD to replicate the DGP output response to monetary policy shock, as opposed to sign restrictions. Specifically, I evaluate the two following structural models:

- *Sign Restrictions*

  This model identifies interest rate shock through sign restrictions on impact responses. Specifically, it employs robust sign restrictions in Table 2. Contractionary interest rate shock reduces inflation rate, consumption growth, investment growth, and hours worked and increases interest rates: $IR^0_{\Delta ci} \leq 0$, $IR^0_{\Delta Ii} \leq 0$,$IR^0_{li} \leq 0$, $IR^0_{\pi i} \leq 0$, $IR^0_{ii} \geq 0$. The object of interest $IR_{\Delta yi}$, i.e, the output response, is left unrestricted.

[12]In models with flexible prices and sticky wages, real wages positively comove contemporaneously with monetary shocks, while in models with sticky prices and flexible wages real wages are negatively related to monetary shock on impact.

[13]For example, see Smets and Wouters (2005) and Smets and Wouters (2007).

- *Bounds on the FEVD*

  Relying on restrictions on the FEVD in Table 2, the FEV of nominal variables is bounded: $0.32 \leq CFEV_i^i(0) \leq 0.77$ and $CFEV_i^\pi(0) \leq 0.27$. Since the object of interest is the real output response, the FEV of real variables is left unbounded. Note that this model satisfies condition (b) in Proposition 3.6, so that characterization of the set does not rely on a specific prior for $\boldsymbol{Q}$.

5.1 Analysis without Estimation Uncertainty

First, I consider analysis without sample bias, or estimation uncertainty, i.e., population analysis. Suppose that there is an infinite amount of data on observables; it implies that the reduced-form VAR is estimated without error and is fixed at values implied by the DGP. As a result, the only unknown object is the matrix $\boldsymbol{A}_0$ in equation (3.1). In order to recover $\boldsymbol{A}_0$, the researcher uses the true covariance matrix $\boldsymbol{\Sigma}$ and identifying restrictions. The setting of this Monte-Carlo experiment isolates the identification uncertainty and excludes sample bias by construction. For each model, Figure 1 reports the DGP output response to (contractionary) monetary policy shock and the 90% range of theory-consistent impulse responses indicating the identification uncertainty. This range is defined by the maximum and minimum response at each horizon; as long as there is no estimation of reduced-form VAR, such a range captures the identification uncertainty implied by each set of identifying restrictions, namely the identified set of the output response.

While sign restrictions are unlikely to provide informative results and recover the theoretical response (panel b), short-run inequality restrictions on the FEVD (panel a) shrink the identified set and are able to pin down the sign of output response. Furthermore, its median replicates the DGP response well, as opposed to sign restrictions.

5.2 Estimation Uncertainty

The previous exercise focuses on uncertainty arising from ability of identifying assumptions to recover the DGP response. There, the VAR coefficient matrices are held fixed at the values implied by the DGP. However, in empirical works these matrices must be estimated from finite samples. Thus, sampling, or estimation, uncertainty is an additional issue to take into account. In order to assess the impact of estimation uncertainty, this Section generates 1000 datasets and set the length of time series to 1000, where the first 800 observations are discarded to remove the impact of initial conditions so that $T^* = 200$ is the artificial sample size, quarterly frequency. At each replication, artificial data are used to estimate the reduced-form VAR from a relatively flat Normal Inverse Wishart distribution.

Figure 2 reports the DGP output response (blue), the identified-set (red) for each model, the average across replications of the median responses (dotted black) and the associated 90% Bayesian credibility region (dashed black). Introduction of estimation uncertainty does not affect the results, in which only the bounds on the FEVD are able to recover the sign of the DGP response. Furthermore, Figure 3 clearly depicts that only the posterior median induced by constraints on the FEVD replicates the DGP response well.[14] Finally, for each replication I compute the error as the difference between the theoretical response and the estimated median response across variables and horizons. I then take the average of the squared errors across replications (MSE) and construct the ratio between the MSE of model with sign restrictions and that with bounds on the FEVD; according to Figure 4, the performance of the latter is superior at any horizons.

Overall, Monte-Carlo exercise shows that constraints on the short-run FEVD shrink the identified set of the output response and fully recover the sign and magnitude of DGP response, as opposed to standard sign restrictions. Next Section evaluates the identification scheme in the data.

6 Empirical Application: Monetary Policy Shocks

A rich literature has studied the impact of monetary policy shocks on output using SVARs, identified with zero restrictions (Christiano, Eichenbaum, and Evans, 1999; Bernanke and Mihov, 1998), sign restrictions (Uhlig, 2005) and both (Arias, Caldara, and Rubio Ramírez, 2018). SVARs identified using zero restrictions have consistently found that a contractionary monetary policy shock implies a significant reduction in short-run real activity. This consensus view has been challenged by Uhlig (2005), who argues against imposing a controversial zero restriction on the IRF of output to a monetary policy shock on impact. Specifically, he identifies a monetary policy shock by imposing sign restrictions only on the IRFs of prices and non-borrowed reserves to this shock, while output response is left unrestricted. The lack of restrictions on output makes this approach appealing and explains its large usage in empirical studies. Remarkably, under this identification scheme, a contractionary monetary policy shock has no significant impact on real variables in the short-run (Uhlig, 2005; Mountford, 2005; Rafiq and

[14]However, a caveat applies; there is huge debate over which measure of central tendency should be used for set-identified SVARs. Common measure is the posterior median, but Fry and Pagan (2011) and Inoue and Kilian (2013) propose alternative measures of point-estimation. Although the problems associated to the posterior median, I employ it as measure of central tendency because it is widely used in empirical works and makes comparison with literature simpler. However, note that using the measures proposed by Fry and Pagan (2011) leaves the results unchanged.

Mallick, 2008) and does not necessarily lead to a decrease in real activity; this result seems to be robust to choice of observables, lag selection, prior specification and sample periods. Furthermore, Arias, Caldara, and Rubio Ramírez (2018) show that identifying restrictions on IRFs à la Uhlig (2005) have counter-intuitive consequences for the systematic response of monetary policy to real output; Antolín-Díaz and Rubio Ramírez (2017) argue that sign restrictions on IRFs yield implausible implications for historical decomposition.

First, this Section illustrates that constraints on the bounds of the FEVD are highly informative and tend to exclude implausible implications by recovering significant effects of monetary policy shocks on real variables (Section 6.1). Second, I compare the results with the inference induced by narrative sign restrictions (Antolín-Díaz and Rubio Ramírez, 2017) and ranking of IRFs (Amir-Ahmadi and Drautzburg, 2018), namely the most recent approaches to sharpen the identification in a sign-restricted model (Section 6.2). Interestingly, theory-driven bounds on the FEVD are more informative, deliver different inference and recover reasonable results for the systematic response of monetary policy equation (Arias, Caldara, and Rubio Ramírez, 2018). Finally, Section 6.3 presents a procedure for model validation using restrictions on the FEVD.

6.1 Seven-Variable SVAR

This Section estimates in the data the two models of the Monte-Carlo exercise and an augmented version of sign restrictions, where the identified shock minimises the FEV contribution to real output growth in the long-run. Among others, this approach dates back to Faust (1998), Sims (1998), and Christiano, Eichenbaum, and Evans (1999), who argue that for every reasonable identification, the monetary policy disturbance needs to explain a small share of the FEV of output in the long-run. In practice, this scheme is implemented by employing Uhlig (2004b) and finding the rotation matrix $\boldsymbol{Q}$ which, among the structural models satisfying the sign restrictions, minimises the FEV of output in the long-run; thus, the model is point-identified.

Models include the same variables as the Monte-Carlo simulation: output growth, consumption growth, investment growth, real wages growth, hours worked, inflation rate, and interest rate. I use the dataset constructed by Stock and Watson (2008). This employs 149 quarterly variables from 1959Q1 to 2008Q4; several of them are monthly and transformed into quarterly by taking averages. In order to get annualized log levels, I take logs and multiply by 4 most of variables, except federal funds rate. Reduced-form prior follows a flat Normal Inverse Wishart distribution.

Figure 5 displays the output responses. Both estimation and inference are dramatically different across set of identifying assumptions: bounds on the FEVD drastically shrink the identified set of output response and lead to informative inference, while sign restrictions support neutrality of monetary policy even in the short-run and are largely uninformative. Although the requirement that the identified shock minimises the FEV contribution to real output growth in the long-run sharpens inference, this still leads to meaningless outcome. Posterior median also differs: it is positive under sign restrictions and augmented sign restrictions, as opposed to the model with theory-driven bounds on the FEVD.

In order to investigate the change in estimation and inference, I study the unbounded FEVD of the sign-restricted SVAR in the data. On impact, $0.00 \leq CFEV_i^{\pi}(0) \leq 0.45$ and $0.00 \leq CFEV_i^{i}(0) \leq 0.55$ with 90% probability; comparison with theory-driven bounds in Table 2 used to enrich sign restrictions shows that the bounds trim the structural parameters implying a high contribution of the shock to variance of inflation rate and low contribution to interest rate fluctuations. Removing such structural models leads to results in Figure 5.

6.2 Comparison with Alternative Methods

Figure 5 confirms that robust constraints on the FEVD lead to estimation and inference dramatically different from sign restrictions. This Section introduces a comparison with alternative schemes of shrinkage in set-identified frameworks. Specifically, most recent and increasingly common benchmarks in the field are restrictions on structural component of monetary policy (Arias, Caldara, and Rubio Ramírez, 2018) and narrative sign restrictions (Antolín-Díaz and Rubio Ramírez, 2017).

Antolín-Díaz and Rubio Ramírez (2017) combine standard sign restrictions with narrative information on the structural shocks and historical decomposition around key historical events. In particular, on top of standard sign restrictions, the model is restricted as follows: the monetary policy shock for the observation corresponding to the last quarter in 1979 must be of positive value (*NSR1*); for the same period, the absolute value of the contribution of monetary policy shocks to the unexpected movement in the federal funds rate is larger than the sum of the absolute value of the contributions of all other structural shocks (*NSR2*). As shown in Figure 6, panel a, in the short-run narrative restrictions are less likely to recover a negative and significant output response, as opposed to constraints on the FEVD; the inference is also dramatically different at longer horizons. Furthermore, second column in Table 3 shows that sign restrictions have 20% probability to violate *NSR1* or *NSR2*, while this probability collapses to 1% with robust bounds on the FEVD. Thus, the latter deliver structural parameters consistent with narrative information in Antolín-Díaz and Rubio Ramírez (2017) without explicitly constraining sign of structural shock and historical decomposition. Note that a caveat applies: original narrative restrictions in Antolín-Díaz and Rubio Ramírez (2017) are applied on monthly data.

Specifically, *NSR1* and *NSR2* have been imposed on October 1979. I have placed them on 1979Q4; however, I have run some robustness checks by slightly varying the restricted quarter and results still hold.

Arias, Caldara, and Rubio Ramírez (2018) achieve set-identification of monetary policy shock by restricting the systematic component of monetary policy, while impulse responses are left unconstrained. The root of this approach dates back to Leeper, Sims, and Zha (1996), Leeper and Zha (2003), and Sims and Zha (2006), who argue that monetary policy choices do not evolve independently of economic conditions, and Taylor (1993), who relates monetary policy changes to output and inflation. Let $\gamma_{\Delta y}, \gamma_{\Delta c}, \gamma_{\Delta I}, \gamma_{\Delta w}, \gamma_l, \gamma_\pi$ denote the contemporaneous reaction of nominal rates to output growth, consumption growth, investment growth, real wages growth, hours worked, and inflation rate, respectively.[15] Constraints on the seven-variable model are the following: $\gamma_{\Delta y} > 0, \gamma_\pi > 0$ and $\gamma_{\Delta c}, \gamma_{\Delta I}, \gamma_{\Delta w}, \gamma_l$ are left unrestricted. Arias, Caldara, and Rubio Ramírez (2018) find that sign restrictions on IRFs tend to violate those restrictions on the structural component of monetary policy with high probability. Table 3 confirms their result, with sign restrictions on IRFs having 71% probability to violate $\gamma_{\Delta y} > 0$ or $\gamma_\pi > 0$. Remarkably, once robust restrictions on the FEVD are taken into account, such a probability drops to 3%. Thus, restrictions on the FEVD tend to eliminate structural parameters which deliver counter-intuitive structural component of monetary policy equation and imply a systematic component of monetary policy in line with Leeper, Sims, and Zha (1996), Leeper and Zha (2003), Sims and Zha (2006), and Taylor (1993) without explicitly constraining the monetary policy equation.

Finally, Amir-Ahmadi and Drautzburg (2018) rank IRFs by magnitude. For identification of monetary policy shock, they enrich sign restrictions by assuming that nominal rates decline for three quarters after the initial shocks. However, and analogous to what they observe for monetary shocks, this strategy does not help and does not sharpen identification induced by sign restrictions; in fact, I find that estimation and inference of output response is the same as sign restrictions in Figure 5, panel b.

6.3 Validation of Theoretical Models

This Section illustrates how to employ robust bounds on the FEVD to contrast competing models in the data when sign restrictions are unable to do so. In literature, sign restrictions are often used for model validation by relying on the methodology in Canova and Paustian (2011): one would derive robust sign restrictions for candidates; estimate SVAR using common sign restrictions and leave unrestricted any response where restrictions differ; select the candidate by

[15] Appendix B provides the exact expression for such parameters.

comparing the estimated SVAR and the restrictions differing in the candidates. An illustrative example is provided by Canova and Paustian (2011): to contrast sticky wages vs. sticky prices framework in the data, they first observe that both models induce common signs on impact response for most variables but real wages. Specifically, sticky wages imply a positive impact response of real wages to contractionary monetary policy, while sticky prices induce a negative response. They then estimate a SVAR in the data identified with common restrictions on all variables but real wages and examine if on impact real wages decrease or go up.

However, sometimes sign restrictions are unable to separate alternative candidates; consider two sub-models of the framework analysed in Section 4.1: M1 ($\xi_p = 0.2$) and M2 ($\xi_p = 0.95$). Table 4, which reports the robust sign restrictions to monetary policy shock for the candidates, shows that it is hard to find sign restrictions which differ in the two sub-models. Specifically, real wage responses cannot be used to validate candidates: M1 is not flexible enough to cause positive real wage responses; M2 would need flexible wages to deliver negative response of real wages. As a result, standard procedure in Canova and Paustian (2011) cannot be employed.[16] Nevertheless, analysis of the theoretical FEVD shows that $CFEV_i^{\pi}(0) \in [0.13, 0.25]$ for M1 and $CFEV_i^{\pi}(0) \in [0.00, 0.03]$ for M2, with 90% probability. I then estimate a SVAR where monetary policy shock is identified with restrictions in Table 4, finding that monetary policy shock explains more than 7% of the inflation error variance on impact. Data seem to reject M2.

Distinguishing between models with different degrees of stickiness may be difficult because they do not necessarily imply differing sign on impact responses; furthermore, formal methods based on likelihood are hardly helpful since stickiness parameters may be weakly identified (Del Negro and Schorfheide, 2008; Canova and Sala, 2009). Thus, FEVD can provide a sound alternative for model validation.

7 Conclusion

Sign-restricted SVARs, which relax exclusion restrictions and rely on weaker assumptions on the sign of impulse responses, are increasingly common. However this minimalist, or agnostic, approach comes at a cost. Sign restrictions will usually deliver a set of structural parameters with very different implications for IRFs, elasticities, historical decomposition or FEVD. On one hand, it is challenging to obtain informative inference and meaningful economic results. On the other hand, some of the admissible structural models may contain implausible implications.

This paper introduces bounds on the FEVD to sharpen identification, reduce the set of admissible structural parameters and remove implausible implications of sign-restricted models.

[16]Looking at sign of responses to shocks other than monetary disturbance does not help either.

First, in a bivariate and trivariate setting, I analytically prove that bounds on the FEVD deliver a strictly smaller set relative to sign restrictions. Interestingly, this also applies to variables not subject to restrictions. For higher dimensional SVARs, I establish necessary conditions when placing bounds on the FEVD leads to a reduced identified set.

Second, the paper also addresses the trade-off between sharp identification and computation and establishes sufficient conditions to determine whether the identified set has positive measure; a correspondent algorithm provides a computationally-fast practical check of the conditions. While recent studies (Giacomini and Kitagawa, 2018; Amir-Ahmadi and Drautzburg, 2018; Gafarov, Meier, and Olea, 2018) establish conditions for non-emptiness under zero and sign restrictions, this paper advances the literature by investigating non-emptiness under bounds on the FEVD.

In order to address the criticism by Baumeister and Hamilton (2015) over the role of prior for $\boldsymbol{Q}$, under a convexity criterion this paper presents a robust-prior procedure through a numerical optimizer, where the identified set, which is constrained by bounds on the FEVD, is distribution-free and does not depend on a specific prior over the rotation matrix. This is line with the proposals in Giacomini and Kitagawa (2018), Gafarov, Meier, and Olea (2018), and Amir-Ahmadi and Drautzburg (2018) for sign and zero restrictions only.

I adapt the procedure in Canova and Paustian (2011) to derive theory-driven bounds on the FEVD, which are consistent with the implications of popular DSGE models, with both real and nominal frictions, and with sufficiently wide ranges for their parameters.

A Monte-Carlo exercise documents effectiveness of those bounds as identifying restrictions in recovering the data-generating process relative to sign restrictions. While sign restrictions typically suggest that contractionary monetary policy shocks have no effects on real variables and are even likely to increase the real activity, an empirical application shows that bounds on the FEVD of inflation and interest rates tend to be highly informative, remove unreasonable effects of monetary shocks on real variables, and sharpen the inference of sign-restricted models. In doing so, the approach here is also more effective than alternative strategies of set-reduction, including long-run equality restrictions on the FEVD (Uhlig, 2004b), narrative sign restrictions (Antolín-Díaz and Rubio Ramírez, 2017), and ranking of IRFs (Amir-Ahmadi and Drautzburg, 2018). It also recovers reasonable signs for the coefficients of the monetary policy equation (Arias, Caldara, and Rubio Ramírez, 2018). Finally, an illustrative example shows how to employ restrictions on the FEVD for model validation.

8 Tables and Figures

Table 1

Parameter	Description	Support
β	Discount factor	$[0.985, 0.995]$
φ	Investment adjustment cost	$[3.00, 8.00]$
σ_c	Inverse of the elasticity of intertemporal substitution for consumption (Risk aversion coefficient)	$[1.00, 5.00]$
λ	Habit parameter	$[0.00, 0.95]$
ξ_w	Wage stickiness	$[0.00, 0.90]$
σ_l	Elasticity of labour supply wrt real wage	$[0.00, 5.00]$
ξ_p	Price stickiness	$[0.00, 0.90]$
ι_w	Indexation in wage setting	$[0.00, 0.80]$
ι_p	Indexation in price setting	$[0.00, 0.80]$
ψ	Capital utility adjustment cost	$[0.00, 1.00]$
Φ	Fixed costs	$[0.50, 2.50]$
r_π	Response to inflation in Taylor rule	$[1.05, 2.50]$
ρ	Interest rate smoothing	$[0.25, 0.95]$
r_Y	Response to output gap in Taylor rule	$[0.00, 0.50]$
$r_{\Delta y}$	Response to change in output gap in Taylor rule	$[0.00, 0.50]$
$\bar{\pi}$	Steady-state inflation rate	$[0.20, 1.00]$
$\bar{l}$	Normalised steady-state hours worked	$[-3.00, 3.00]$
$\bar{\gamma}$	Steady-state growth rate	$[0.20, 0.60]$
α	Share of the capital in production	$[0.30, 0.40]$
ρ_a	Persistence of productivity disturbances	$[0.50, 0.99]$
ρ_b	Persistence of risk premium disturbance	$[0.00, 0.50]$
ρ_g	Persistence of spending disturbances	$[0.50, 0.99]$
ρ_i	Persistence of investment-specific disturbances	$[0.20, 0.99]$
ρ_r	Persistence of monetary policy disturbances	$[0.00, 0.50]$
ρ_p	Persistence of price mark-up disturbances	$[0.50, 0.99]$
ρ_w	Persistence of wage mark-up disturbances	$[0.50, 0.99]$
ρ_{ga}	Persistence of productivity disturbances on spending	$[0.00, 0.99]$
μ_p	MA term in price mark-up disturbance	$[0.30, 0.99]$
μ_w	MA term in wage mark-up disturbance	$[0.40, 0.99]$

The disturbances are: technology shock ($\epsilon_t^a = \rho_a \epsilon_{t-1}^a + \eta_t^a, \eta_t^a \sim N(0, \sigma_a^2)$); risk premium shock ($\epsilon_t^b = \rho_b \epsilon_{t-1}^b + \eta_t^b, \eta_t^b \sim N(0, \sigma_b^2)$); investment-specific technology shock ($\epsilon_t^i = \rho_i \epsilon_{t-1}^i + \eta_t^i, \eta_t^i \sim N(0, \sigma_i^2)$); wage mark-up shock ($\epsilon_t^w = \rho_w \epsilon_{t-1}^w + \eta_t^w - \mu_w \eta_{t-1}^w, \eta_t^w \sim N(0, \sigma_w^2)$); price mark-up shock ($\epsilon_t^p = \rho_p \epsilon_{t-1}^p + \eta_t^p - \mu_p \eta_{t-1}^p, \eta_t^p \sim N(0, \sigma_p^2)$); exogenous spending shock ($\epsilon_t^g = \rho_g \epsilon_{t-1}^g + \eta_t^g + \rho_{ga} \eta_t^a, \eta_t^g \sim N(0, \sigma_g^2)$); monetary policy shock ($\epsilon_t^r = \rho_r \epsilon_{t-1}^r + \eta_t^r, \eta_t^r \sim N(0, \sigma_r^2)$). The following parameters are held fixed: $\delta = 0.025, g_y = 0.18, \phi_w = 1.5, \epsilon_p = 10, \epsilon_w = 10$, namely the depreciation rate, spending-output ratio, the steady-state mark-up in the labour market, the Kimball aggregators in the goods and labour market, respectively.

Table 2

	Δy_t	Δc_t	ΔI_t	Δw_t	l_t	π_t	i_t
IRFs, $h = 0$	-	-	-	?	-	-	+
FEV, $h = 0$	$[0.00, 0.25]$	$[0.01, 0.20]$	$[0.01, 0.19]$	$[0.00, 0.06]$	$[0.01, 0.12]$	$[0.00, 0.27]$	$[0.32, 0.77]$

Sign of impact responses and FEV at horizon $h = 0$ to contractionary monetary policy shock, framework in Section 4.1. $+(-)$ indicate that a certain variable has the 90% probability to response positively (negatively) on impact; ? indicates that the sign of the response cannot uniquely pinned down; the bounds of the FEV represent the 5% and 95% percentiles.

Table 3

Probability	Pr(violation of *NSR1* $\cup$ *NSR2*)	$\Pr(\gamma_{\Delta y} < 0)$	$\Pr(\gamma_{\pi} < 0)$	$\Pr(\gamma_{\Delta y} < 0 \cup \gamma_{\pi} < 0)$
Sign Restrictions	0.20	0.71	0.15	0.77
Restrictions on the FEV	0.01	0.03	0.02	0.04

Empirical application: the entries denote the individual and joint probabilities of two identification strategies (sign restrictions and restrictions on the FEV) of violating narrative sign restrictions (second column) and restrictions on the coefficients of the monetary policy equation (third, fourth and fifth column). Probabilities are computed as the share of structural parameters draws which violate the correspondent restrictions. See Section 6.2 for details.

Table 4

	Δy_t	Δc_t	ΔI_t	Δw_t	l_t	π_t	i_t
M1	-	-	-	?	-	-	+
M2	-	-	-	?	-	-	+

Model validation: sign of impact responses to contractionary monetary policy shock for M1 and M2 as defined in Section 6.3. $+(-)$ indicate that a certain variable has the 90% probability to response positively (negatively) on impact; ? indicates that the sign of the response cannot uniquely pinned down.

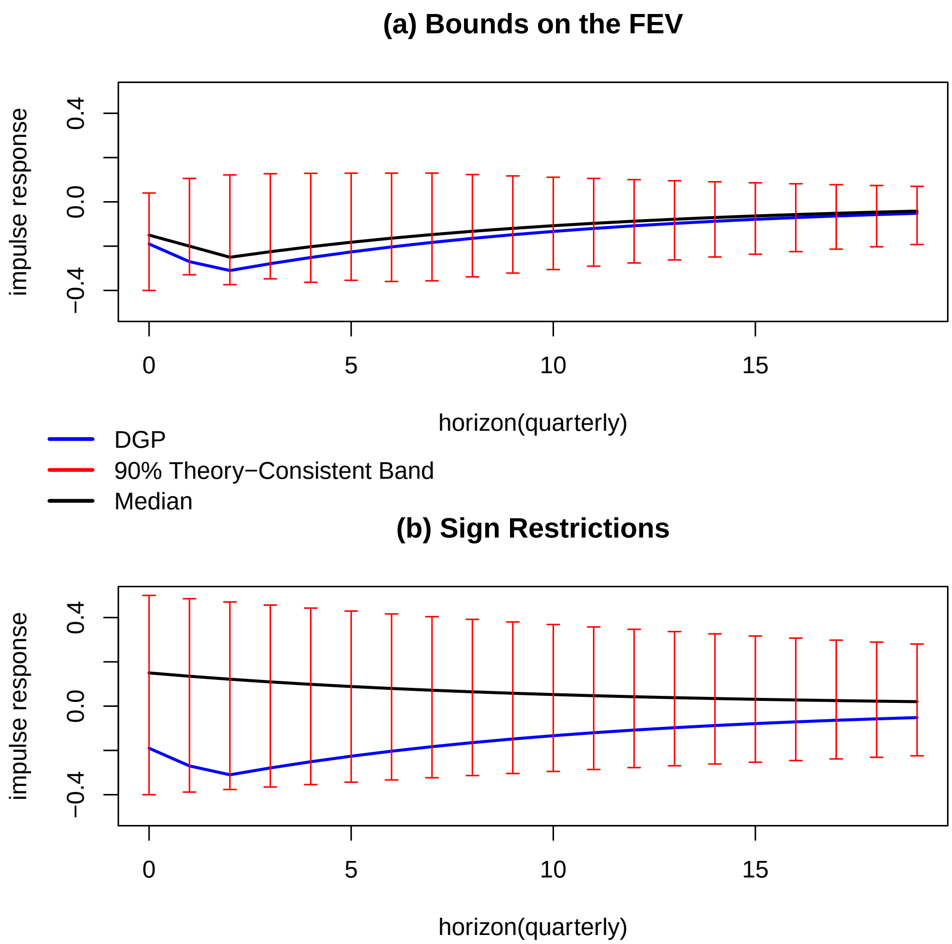

Figure 1: Population Analysis, Monte-Carlo Simulation

Figure 1 reports the theoretical DGP output response (blue line) to contractionary monetary policy shock and the 90% range of theory-consistent responses (red vertical bars). See Section 5 for details. The shock size is set to one standard deviation.

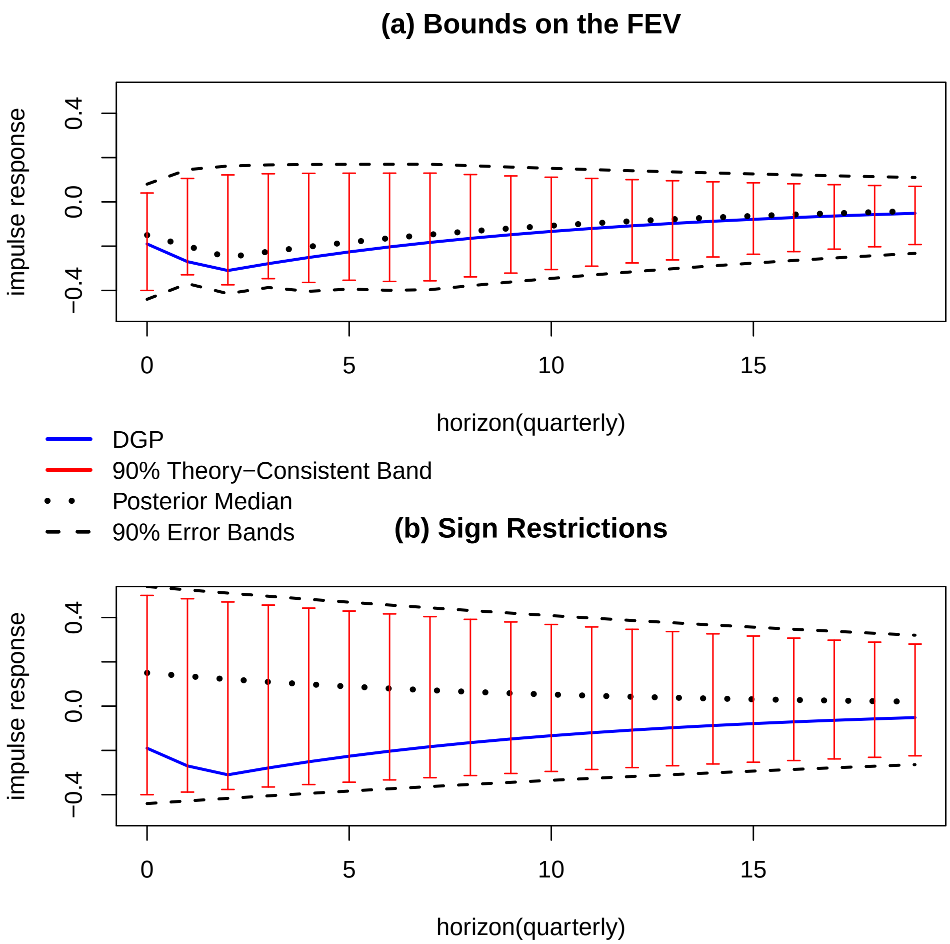

Figure 2: Sample Analysis, Monte-Carlo Simulation

Figure 2 reports the theoretical DGP output response (blue line) to contractionary monetary policy shock, the 90% range of theory-consistent responses (red vertical bars), the posterior median (black dotted line) and the associated 90% Bayesian credibility region (black dashed lines). See Section 5 for details. The shock size is set to one standard deviation.

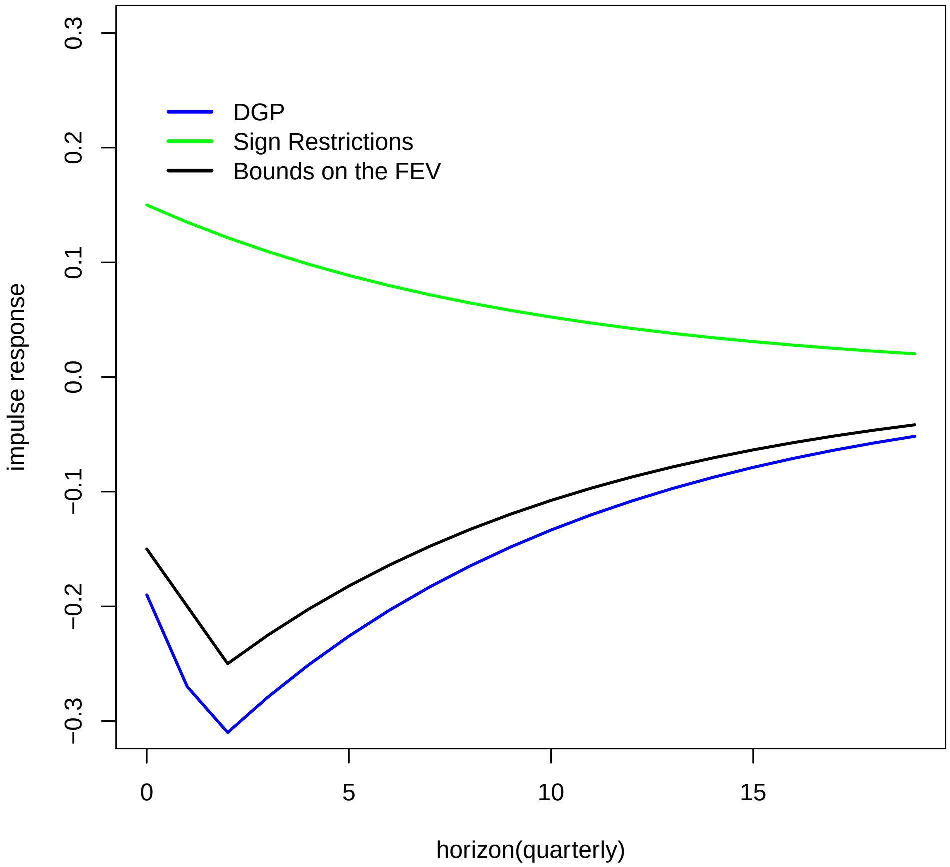

Figure 3: Posterior Medians, Monte-Carlo Simulation

Figure 3 reports the theoretical DGP output response (blue line) to contractionary monetary policy shock, the posterior median induced by inequality restrictions on the FEV (black line), and by sign restrictions (green line). See Section 5 for details. The shock size is set to one standard deviation.

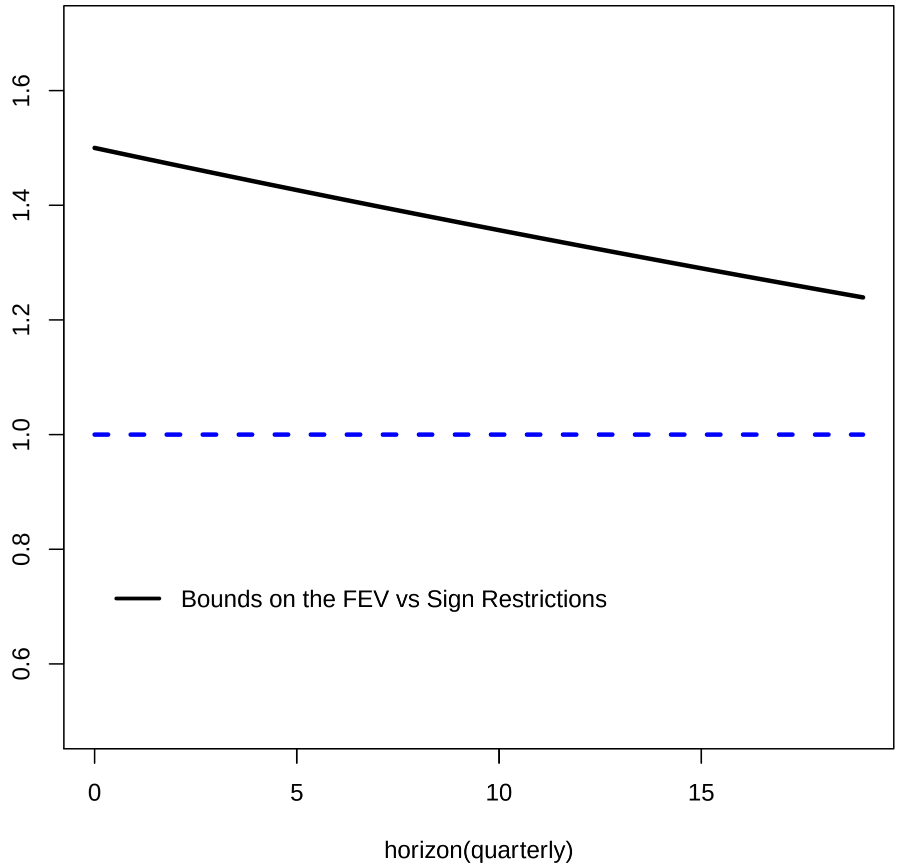

Figure 4: Mean Square Error, Monte-Carlo Simulation

The black line reports the ratio of the Mean Squared Error (MSE) between the model with sign restrictions and that with inequality restrictions on the FEV. Dashed blue line is fixed at 1. For details about the computation of the MSE, see Section 5.

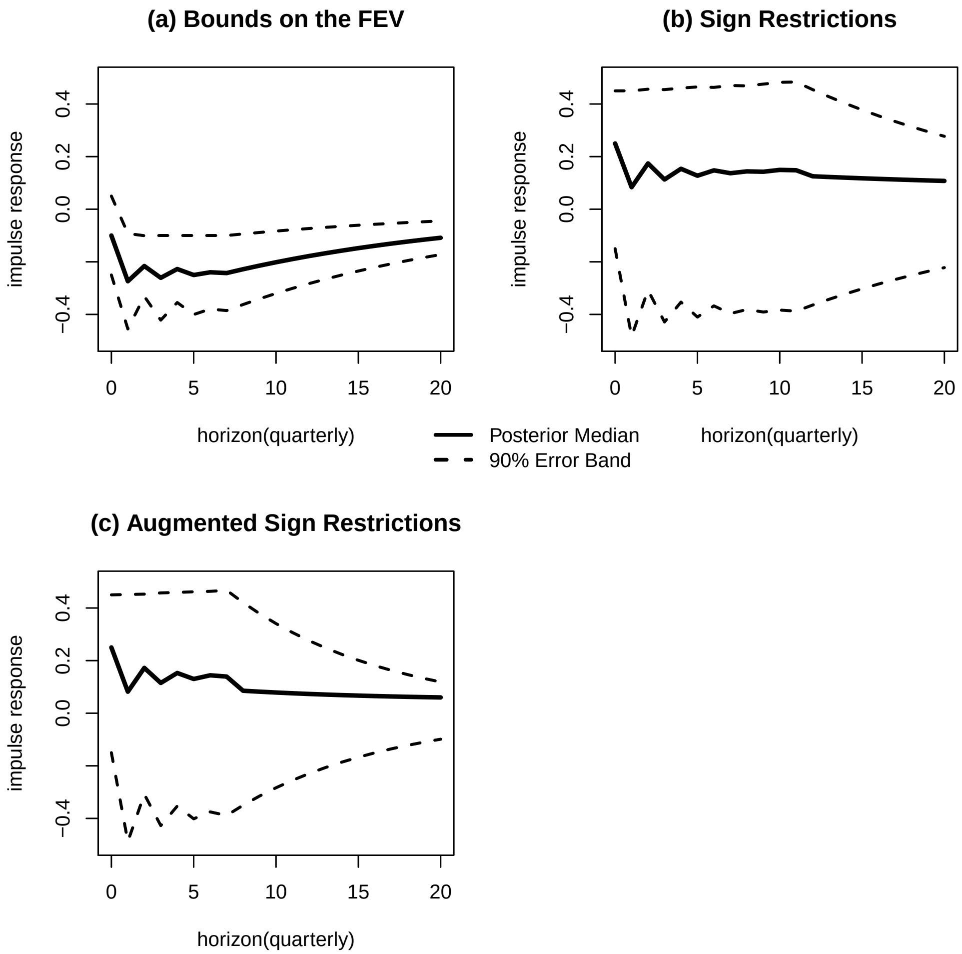

Figure 5: Output Impulse Responses, Empirical Application

In each panel, the solid lines plot the posterior median and the dashed black lines show the correspondent 90% Bayesian credibility region. Shock size is set to one standard deviation.

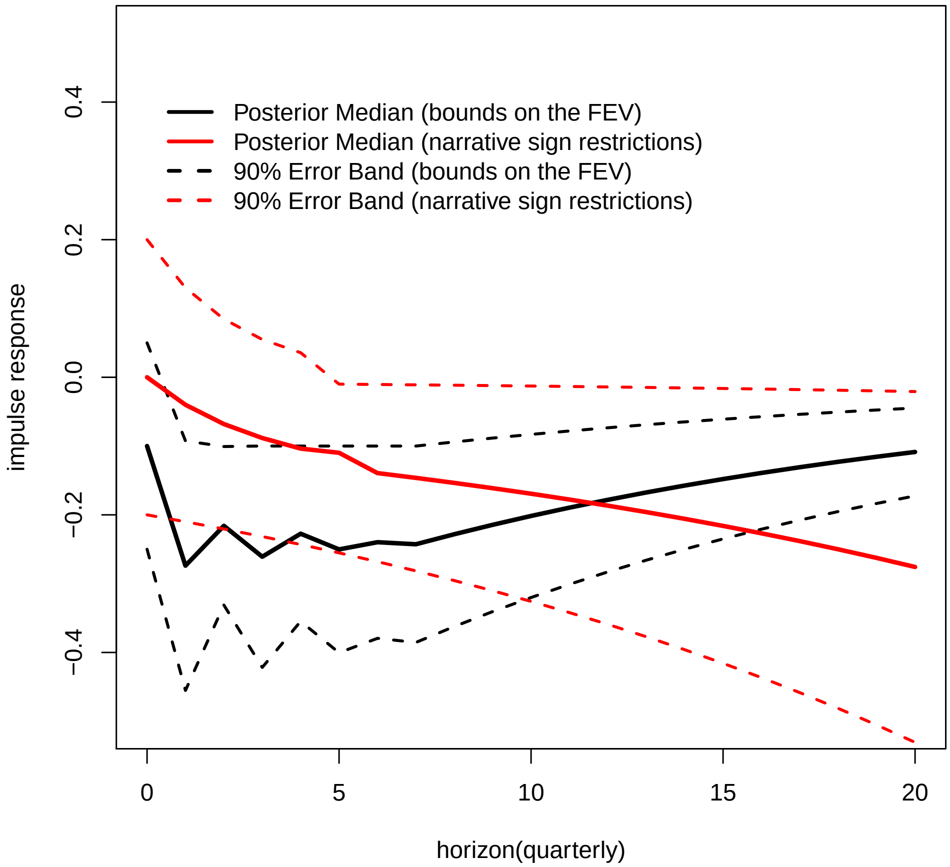

Figure 6: Output Impulse Responses, Empirical Application: Bounds on the FEV and Narrative Sign Restrictions.

Solid and dashed black lines denote the posterior median and the 90% Bayesian credibility region induced by bounds restrictions on the FEV, respectively. Dashed red lines represent the 90% Bayesian credibility region induced by narrative sign restrictions.

References

Amir-Ahmadi, P., and T. Drautzburg (2018): "Identification through heterogeneity," *Unpubloshed Manuscript.*

Antolín-Díaz, J., and J. Rubio Ramírez (2017): "Narrative sign restrictions for SVARs," *American Economic Review, Forthcoming.*

Arias, J., D. Caldara, and J. Rubio Ramírez (2018): "The systematic component of monetary policy in SVARs: an agnostic identification procedure," *Journal of Monetary Economics, Accepted.*

Arias, J. E., J. F. Rubio-Ramirez, and D. Waggoner (2017): "Inference based on SVARs identified with sign and zero restrictions: theory and applications," *Federal Reserve Bank of Atlanta Working Paper Series.*

Baumeister, C., and J. D. Hamilton (2015): "Sign restrictions, structural vector autoregressions, and useful prior information," *Econometrica*, 83(5), 1963–1999.

Bernanke, B. S., and I. Mihov (1998): "Measuring monetary policy," *The Quarterly Journal of Economics*, 113(3), 869–902.

Blanchard, O. J., and D. Quah (1989): "The dynamic effects of aggregate demand and supply disturbances," *American Economic Review*, 79(4), 655.

Canova, F., and G. D. Nicolo (2002): "Monetary disturbances matter for business fluctuations in the G-7," *Journal of Monetary Economics*, 49(6), 1121–1159.

Canova, F., and M. Paustian (2011): "Business cycle measurement with some theory," *Journal of Monetary Economics*, 58(4), 345–361.

Canova, F., and L. Sala (2009): "Back to square one: Identification issues in DSGE models," *Journal of Monetary Economics*, 56(4), 431–449.

Castelnuovo, E. (2015): "Monetary policy neutrality? Sign restrictions go to Monte Carlo," *unpublished manuscript.*

Christiano, L. J., M. Eichenbaum, and C. L. Evans (1999): "Monetary policy shock: what have we learned and to what end?," in *Handbook of Macroeconomics*, ed. by J. B. Taylor, and M. Woodford. Elsevier.

Dedola, L., and S. Neri (2007): "What does a technology shock do? A VAR analysis with model-based sign restrictions," *Journal of Monetary Economics*, 54(2), 512–549.

Dedola, L., G. Rivolta, and L. Stracca (2017): "If the Fed sneezes, who catches a cold?," *Journal of International Economics*, 108(Supplement 1), S23–S41.

Del Negro, M., and F. Schorfheide (2008): "Forming priors for DSGE models (and how it affects the assessment of nominal rigidities)," *Journal of Monetary Economics*, 55(7), 1191–1208.

DiTraglia, F., and C. García-Jimeno (2016): "A framework for eliciting, incorporating, and disciplining identification beliefs in linear models," *NBER Working Paper Series*.

Faust, J. (1998): "The robustness of identified VAR conclusions about money," *Carnegie-Rochester Conference Series on Public Policy*, 48, 207–244.

Fry, R., and A. Pagan (2011): "Sign restrictions in structural vector autoregressions: A critical review," *Journal of Economic Literature*, 49(4), 938–960.

Fujita, S. (2011): "Dynamics of worker flows and vacancies: evidence from the sign restriction approach," *Journal of Applied Econometrics*, 26(1), 89–121.

Gafarov, B., M. Meier, and J. L. M. Olea (2018): "Delta-Method inference for a class of set-identified SVARs," *Journal of Econometrics*, 203(2), 316–327.

Giacomini, R., and T. Kitagawa (2018): "Robust inference about partially-identified SVARs," *Cemmap Working Paper*.

Inoue, A., and L. Kilian (2013): "Inference on impulse response functions in structural VAR models," *Journal of Econometrics*, 177(1), 1–13.

Kilian, L., and D. Murphy (2012): "Why agnostic sign restrictions are not enough: understanding the dynamics of oil market VAR models," *Journal of the European Economic Association*, 10(5), 1166–1188.

Leeper, E., C. Sims, and T. Zha (1996): "What does monetary policy do?," *Brookings Papers on Economic Activity*, 2, 1–78.

Leeper, E. M., and T. Zha (2003): "Modest policy interventions," *Journal of Monetary Economics*, 50(8), 1673–1700.

Lippi, F., and A. Nobili (2012): "Oil and the macroeconomy: a quantitative structural analysis," *Journal of the European Economic Association*, 10(5), 1059–1083.

Mountford, A. (2005): "Leaning into the wind: a structural VAR investigation of UK Monetary Policy," *Oxford Bulletin of Economics and Statistics*, 67(5), 597–621.

Pappa, E. (2009): "The effects of fiscal shocks on employment and the real wage," *International Economic Review*, 50(1), 217–244.

Paustian, M. (2007): "Assessing sign restrictions," *The BE Journal of Macroeconomics*, 7(1), Article 23.

Peersman, G., and R. Straub (2009): "Technology shocks and robust sign restrictions in a Euro Area SVAR," *International Economic Review*, 50(3), 727–750.

Rafiq, S., and S. Mallick (2008): "The effect of monetary policy on output in EMU3: a sign restriction approach," *Journal of Macroeconomics*, 30(4), 1756–1791.

Rothenberg, T. J. (1971): "Identification in parametric models," *Econometrica: Journal of the Econometric Society*, pp. 577–591.

Rubio-Ramirez, J., D. Waggoner, and T. Zha (2010): "Structural vector autoregressions: theory of identification and algorithm for inference," *The Review of Economic Studies*, 77(2), 665–696.

Scholl, A., and H. Uhlig (2008): "New evidence on the puzzles: results from agnostic identification on monetary Policy and exchange Rates," *Journal of International Economics*, 76(1), 1–13.

Schorfheide, F. (2016): "Macroeconometrics - A Discussion," Discussion paper.

Sims, C. (1980): "Macroeconomics and reality," *Econometrica*, 48(1), 1–48.

Sims, C., and T. Zha (2006): "Does monetary policy generate recessions?," *Macroeconomic Dynamics*, 10, 231–272.

Sims, C. A. (1998): "Comment on Glenn Rudebusch's" Do measures of monetary policy in a VAR make sense?"," *International Economic Review*, 39(4), 933–941.

Smets, F., and R. Wouters (2003): "An estimated dynamic stochastic general equilibrium model of the euro area," *Journal of the European economic association*, 1(5), 1123–1175.

——— (2005): "Comparing shocks and frictions in US and euro area business cycles: a Bayesian DSGE approach," *Journal of Applied Econometrics*, 20(2), 161–183.

Smets, F., and R. Wouters (2007): "Shocks and frictions in US business cycles: A Bayesian DSGE approach," *American economic review*, 97(3), 586–606.

Stock, J. H., and M. Watson (2008): "Forecasting in dynamic factor models subject to structural instability," in *The Methodology and Practice of Econometrics. A Festschrift in Honour of David F. Hendry*, ed. by J. Castle, and N. Shephard. Oxford University Press.

Taylor, J. B. (1993): "Discretion versus policy rules in practice," in *Carnegie-Rochester conference series on public policy*, vol. 39, pp. 195–214. Elsevier.

Uhlig, H. (2004a): "Do technology shocks lead to a fall in total hours worked?," *Journal of the European Economic Association*, 2(2-3), 361–371.

——— (2004b): "What moves GNP?," in *Econometric Society 2004 North American Winter Meetings*, no. 636. Econometric Society.

Uhlig, H. (2005): "What are the effects of monetary policy on output? Results from an agnostic identification procedure," *Journal of Monetary Economics*, 52(2), 381–419.

Uhlig, H. (2017): "Shocks, Sign Restrictions, and Identification," in *Advances in Economics and Econometrics: Volume 2: Eleventh World Congress*, vol. 2, p. 95. Cambridge University Press.

Vargas-Silva, C. (2008): "Monetary policy and the US housing market: A VAR analysis imposing sign restrictions," *Journal of Macroeconomics*, 30(3), 977–990.

Appendices

A Omitted Proofs

A.1 Bivariate Setting

Proposition 3.1.

This proof proceeds as follows: first, it derives the identified sets in (3.7) and (3.8); it then compares the two sets.

Following Uhlig (2005), $\boldsymbol{A}_0$ can be parametrized via the Cholesky matrix $\boldsymbol{\Sigma}_{tr}$ and a rotation matrix $\boldsymbol{Q} = \begin{pmatrix} \cos\rho & -\sin\rho \\ \sin\rho & \cos\rho \end{pmatrix}$ with spherical coordinate $\rho \in [0, 2\pi]$. The structural matrix of impact responses can be written as

$$\boldsymbol{IR}^0 = \boldsymbol{A}_0^{-1} = \boldsymbol{\Sigma}_{tr}\boldsymbol{Q} = \begin{pmatrix} \sigma_{11}\cos\rho & -\sigma_{11}\sin\rho \\ \sigma_{21}\cos\rho + \sigma_{22}\sin\rho & -\sigma_{21}\sin\rho + \sigma_{22}\cos\rho \end{pmatrix}$$

and the parameter of interest is $\alpha \equiv \sigma_{11}\cos\rho$, where $\boldsymbol{\phi} = (\sigma_{11}, \sigma_{21}, \sigma_{22}) \in \boldsymbol{\Phi} = \mathbb{R}_+ \times \mathbb{R} \times \mathbb{R}_+$. Following Christiano, Eichenbaum, and Evans (1999), I impose the sign normalization restrictions by constraining the diagonal elements of $\boldsymbol{A}_0$ to being nonnegative,

$$\sigma_{22}\cos\rho - \sigma_{21}\sin\rho \geq 0 \tag{A.1}$$

and

$$\sigma_{11}\cos\rho \geq 0. \tag{A.2}$$

The identifying sign restrictions *SR1* and *SR2* in Section 3.2.1 are expressed as

$$\sigma_{11}\sin\rho \geq 0, \tag{A.3}$$

$$-\sigma_{22}\sin\rho - \sigma_{21}\cos\rho \leq 0. \tag{A.4}$$

Given $\boldsymbol{\phi}$, the identified set for $\alpha = \sigma_{11}\cos\rho$ is given by its range as ρ varies over the range characterized by the restrictions (A.1) - (A.4).

Assume $\sigma_{21} > 0$. Constraints (A.2) and (A.3) induce $\rho \in [0, \frac{\pi}{2}]$; constraints (A.1) and (A.4) imply $\rho \in [\arctan(-\sigma_{21}/\sigma_{22}), \arctan(\sigma_{22}/\sigma_{21})]$. Intersecting the two intervals leads to $[0, \arctan(\sigma_{22}/\sigma_{21})]$ as the identified set for ρ. Thus, for $\sigma_{21} > 0$ the identified set for α in (3.7) follows. A similar argument applies for $\sigma_{21} \leq 0$:

$$IS_\alpha(\boldsymbol{\phi}) \equiv \begin{cases} \left[\sigma_{11}\cos\left(\arctan\left(\frac{\sigma_{22}}{\sigma_{21}}\right)\right), \sigma_{11}\right], & \text{for } \sigma_{21} > 0, \\ \left[0, \sigma_{11}\cos\left(\arctan\left(-\frac{\sigma_{21}}{\sigma_{22}}\right)\right)\right], & \text{for } \sigma_{21} \leq 0. \end{cases} \tag{A.5}$$

FEVR assumes that the contribution of shock ϵ_2 to the total error variance of y_1 is bounded between $\underline{k}$ and $\bar{k}$. Following the notation introduced in Section 3, this restriction can be written as

$$\underline{k} \leq CFEV_{\epsilon_2}^{y_1}(0) = \frac{FEV_{\epsilon_2}^{y_1}(0)}{FEV^{y_1}(0)} \leq \bar{k}, \tag{A.6}$$

where $0 \leq \underline{k} < \bar{k} \leq 1$. Given specification of $\boldsymbol{IR}^0$, note that

$$FEV^{y_1}_{\epsilon_2}(0) = \sigma_{11} \sin^2 \rho,$$
$$FEV^{y_1}(0) = \sigma_{11}^2 \sin^2 \rho + \sigma_{11}^2 \cos^2 \rho = \sigma_{11}^2.$$

Thus, restriction (A.6) can be written as

$$\underline{k} \leq \sin^2 \rho \leq \bar{k} \tag{A.7}$$

and imposes quadratic constraints on $\boldsymbol{Q}$. Under constraints (A.1) - (A.4) and (A.7), the argument used above leads to the identified set for α in (3.8):

$$IS_\alpha(\boldsymbol{\phi}) \equiv \begin{cases} \left[\sigma_{11}\cos(\arcsin\sqrt{\bar{k}}), \sigma_{11}\cos(\arcsin\sqrt{\underline{k}})\right] \\ \text{for } \{\sigma_{21} > 0, \bar{k} < \bar{k}^*\} \cup \{\sigma_{21} \leq 0, \underline{k} > \underline{k}^*\}, \\ \left[\sigma_{11}\cos\left(\arctan\left(\frac{\sigma_{22}}{\sigma_{21}}\right)\right), \sigma_{11}\cos(\arcsin\sqrt{\underline{k}})\right] \\ \text{for } \sigma_{21} > 0, \bar{k} \geq \bar{k}^*, \\ \left[\sigma_{11}\cos(\arcsin\sqrt{\bar{k}}), \sigma_{11}\cos\left(\arctan\left(-\frac{\sigma_{21}}{\sigma_{22}}\right)\right)\right] \\ \text{for } \sigma_{21} \leq 0, \underline{k} \leq \underline{k}^*, \end{cases} \tag{A.8}$$

where $\bar{k}^* = \sin^2(\arctan(\frac{\sigma_{22}}{\sigma_{21}}))$, $\underline{k}^* = \sin^2(\arctan(-\frac{\sigma_{21}}{\sigma_{22}}))$.

First, assume that $\underline{k} \neq 0$, $\bar{k} \neq 1$, i.e., both lower and upper bounds in (A.7) are constrained. For $\sigma_{21} > 0$, $\bar{k} < \bar{k}^*$, $IS_\alpha(\boldsymbol{\phi})$ in (A.8) is strictly smaller than $IS_\alpha(\boldsymbol{\phi})$ in (A.5) because $\sigma_{11}\cos(\arcsin\sqrt{\underline{k}}) < \sigma_{11}$ and $\sigma_{11}\cos(\arcsin\sqrt{\bar{k}}) > \sigma_{11}\cos\left(\arctan\left(\frac{\sigma_{22}}{\sigma_{21}}\right)\right)$. For $\sigma_{21} \leq 0, \underline{k} > \underline{k}^*$, the reduction in the identified set follows from the fact that $\sigma_{11}\cos(\arcsin\sqrt{\bar{k}}) > 0$ and $\sigma_{11}\cos(\arcsin\sqrt{\underline{k}}) < \sigma_{11}\cos\left(\arctan\left(-\frac{\sigma_{21}}{\sigma_{22}}\right)\right)$. The same argument applies under $\sigma_{21} > 0, \bar{k} \geq \bar{k}^*$ and $\sigma_{21} \leq 0, \underline{k} \leq \underline{k}^*$.

Second, suppose that $\underline{k} = 0, \bar{k} \neq 1$, i.e., the lower bound of constraint (A.7) is unrestricted. The identified set in (A.8) then becomes

$$IS_\alpha(\boldsymbol{\phi}) \equiv \begin{cases} \left[\sigma_{11}\cos(\arcsin\sqrt{\bar{k}}), \sigma_{11}\right] \\ \text{for } \sigma_{21} > 0, \bar{k} < \bar{k}^*, \\ \left[\sigma_{11}\cos\left(\arctan\left(\frac{\sigma_{22}}{\sigma_{21}}\right)\right), \sigma_{11}\right] \\ \text{for } \sigma_{21} > 0, \bar{k} \geq \bar{k}^*, \\ \left[\sigma_{11}\cos(\arcsin\sqrt{\bar{k}}), \sigma_{11}\cos\left(\arctan\left(-\frac{\sigma_{21}}{\sigma_{22}}\right)\right)\right] \\ \text{for } \sigma_{21} \leq 0. \end{cases} \tag{A.9}$$

For $\sigma_{21} > 0, \bar{k} \geq \bar{k}^*$, $IS_\alpha(\boldsymbol{\phi})$ in (A.9) is equivalent to $IS_\alpha(\boldsymbol{\phi})$ in (A.5); otherwise, the identified set in (A.9) is strictly smaller.

Finally, assume that $\underline{k} \neq 0, \bar{k} = 1$, i.e., the upper bound in (A.7) is unconstrained. The identified set in (A.8) is now

$$IS_\alpha(\boldsymbol{\phi}) \equiv \begin{cases} \left[\sigma_{11} \cos\left(\arctan\left(\frac{\sigma_{22}}{\sigma_{21}}\right)\right), \sigma_{11} \cos(\arcsin\sqrt{\underline{k}})\right] \\ \text{for } \sigma_{21} > 0, \\ \left[0, \sigma_{11} \cos(\arcsin\sqrt{\underline{k}})\right] \\ \text{for } \sigma_{21} \leq 0, \underline{k} > \underline{k}^*, \\ \left[0, \sigma_{11} \cos\left(\arctan\left(-\frac{\sigma_{21}}{\sigma_{22}}\right)\right)\right] \\ \text{for } \sigma_{21} \leq 0, \underline{k} \leq \underline{k}^*. \end{cases} \tag{A.10}$$

For $\sigma_{21} \leq 0, \underline{k} \leq \underline{k}^*$, $IS_\alpha(\boldsymbol{\phi})$ in (A.10) is equivalent to $IS_\alpha(\boldsymbol{\phi})$ in (A.5); otherwise, the identified set in (A.10) is strictly smaller.

■

Proposition 3.2.

FEVR2 assumes that the contribution of shock ϵ_1 to the total error variance of y_2 is bounded between $\underline{k}$ and $\bar{k}$. Following the notation introduced in Section 3, this restriction can be written as

$$\underline{k} \leq CFEV_{\epsilon_1}^{y_2}(0) = \frac{FEV_{\epsilon_1}^{y_2}(0)}{FEV^{y_2}(0)} \leq \bar{k}, \tag{A.11}$$

where $0 \leq \underline{k} < \bar{k} \leq 1$. Given specification of $\boldsymbol{IR}^0$, note that

$$FEV_{\epsilon_1}^{y_2}(0) = (\sigma_{21} \cos\rho + \sigma_{22} \sin\rho)^2,$$
$$FEV^{y_2}(0) = \sigma_{21}^2 + \sigma_{22}^2.$$

Thus, restriction (A.6) can be written as

$$\underline{k} \leq \frac{(\sigma_{21} \cos\rho + \sigma_{22} \sin\rho)^2}{\sigma_{21}^2 + \sigma_{22}^2} \leq \bar{k}. \tag{A.12}$$

The argument in the previous proof delivers Proposition 3.2. ■

A.2 Trivariate Setting

Proposition 3.3.

This proof first derives the identified sets in (3.10) and (3.11) and then makes the comparison.

In the trivariate setting, $\boldsymbol{Q}$ can be written as the product of three Givens matrices $\boldsymbol{Q}_{12}$, $\boldsymbol{Q}_{13}$ and $\boldsymbol{Q}_{23}$, each rotating a different pair of columns of the matrix to be transformed:

$$\boldsymbol{Q} = \begin{pmatrix} \cos\rho_{12} & -\sin\rho_{12} & 0 \\ \sin\rho_{12} & \cos\rho_{12} & 0 \\ 0 & 0 & 1 \end{pmatrix} \begin{pmatrix} \cos\rho_{13} & 0 & -\sin\rho_{13} \\ 0 & 1 & 0 \\ \sin\rho_{13} & 0 & \cos\rho_{13} \end{pmatrix} \begin{pmatrix} 1 & 0 & 0 \\ 0 & \cos\rho_{23} & -\sin\rho_{23} \\ 0 & \sin\rho_{23} & \cos\rho_{23} \end{pmatrix}$$

For simplicity, the main text limits the analysis to the case where $\rho_{12} = \rho_{23} = 0$, namely $\boldsymbol{Q}_{12} = \boldsymbol{Q}_{23} = \boldsymbol{I}_3$, $\boldsymbol{Q} = \boldsymbol{Q}_{13}$ and $\rho = \rho_{13}$. Thus, there are the following sign normalizations:

$$\sigma_{11}\cos\rho \geq 0, \tag{A.13}$$

$$\sigma_{22} \geq 0, \tag{A.14}$$

which is always satisfied, and

$$-\sigma_{31}\sin\rho + \sigma_{33}\cos\rho \geq 0. \tag{A.15}$$

The identifying sign restrictions *SR1*, *SR2* and *SR3* in Section 3.2.2 are

$$\sigma_{11}\sin\rho \geq 0 \tag{A.16}$$

$$\sigma_{21}\cos\rho \geq 0, \tag{A.17}$$

$$\sigma_{31}\cos\rho + \sigma_{33}\sin\rho \geq 0. \tag{A.18}$$

Under constraints (A.13) - (A.18), the argument used for Proposition 3.1 leads to the identified set for $\alpha \equiv \sigma_{11}\cos\rho$ in (3.11):

$$IS_\alpha(\boldsymbol{\phi}) \equiv \begin{cases} \left[\sigma_{11}\cos\left(\arctan\left(\frac{\sigma_{33}}{\sigma_{31}}\right)\right), \sigma_{11}\right], & \text{for } \sigma_{31} > 0, \\ \left[0, \sigma_{11}\cos\left(\arctan\left(-\frac{\sigma_{31}}{\sigma_{33}}\right)\right)\right], & \text{for } \sigma_{31} \leq 0, \end{cases} \tag{A.19}$$

where sign restrictions are defined if and only if $\sigma_{21} \geq 0$.

FEVR3 assumes that the contribution of shock ϵ_3 to the total error variance of y_2 is bounded between $\underline{k}$ and $\bar{k}$. This restriction can be written as

$$\underline{k} \leq CFEV_{\epsilon_3}^{y_2}(0) = \frac{FEV_{\epsilon_3}^{y_2}(0)}{FEV^{y_2}(0)} \leq \bar{k}, \tag{A.20}$$

where $0 \leq \underline{k} < \bar{k} \leq 1$. Given specification of $\boldsymbol{IR}^0$, note that

$$FEV_{\epsilon_3}^{y_2}(0) = \sigma_{21}^2\sin^2\rho,$$
$$FEV^{y_2}(0) = \sigma_{21}^2 + \sigma_{22}^2.$$

Thus, restriction (A.20) can be written as

$$\underline{k} \leq \frac{\sigma_{21}^2 \sin^2 \rho}{\sigma_{21}^2 + \sigma_{22}^2} \leq \bar{k}. \tag{A.21}$$

Constraints (A.13) - (A.18) and (A.21) yields the identified set in (3.11):

$$IS_\alpha(\boldsymbol{\phi}) \equiv \begin{cases} \left[\sigma_{11}\cos\left(\arcsin\left(\frac{\sqrt{\bar{k}(\sigma_{21}^2+\sigma_{22}^2)}}{\sigma_{21}}\right)\right), \sigma_{11}\cos\left(\arcsin\left(\frac{\sqrt{\underline{k}(\sigma_{21}^2+\sigma_{22}^2)}}{\sigma_{21}}\right)\right)\right], \\ \text{for } \{\sigma_{31} > 0, \bar{k} < \bar{k}^*\} \cup \{\sigma_{31} \leq 0, \underline{k} > \underline{k}^*\}, \\ \left[\sigma_{11}\cos\left(\arctan\left(\frac{\sigma_{33}}{\sigma_{31}}\right)\right), \sigma_{11}\cos\left(\arcsin\left(\frac{\sqrt{\underline{k}(\sigma_{21}^2+\sigma_{22}^2)}}{\sigma_{21}}\right)\right)\right], \\ \text{for } \sigma_{31} > 0, \bar{k} \geq \bar{k}^*, \\ \left[\sigma_{11}\cos\left(\arcsin\left(\frac{\sqrt{\bar{k}(\sigma_{21}^2+\sigma_{22}^2)}}{\sigma_{21}}\right)\right), \sigma_{11}\cos\left(\arctan\left(-\frac{\sigma_{31}}{\sigma_{33}}\right)\right)\right], \\ \text{for } \sigma_{31} \leq 0, \underline{k} \leq \underline{k}^*, \end{cases} \tag{A.22}$$

where $\underline{k}^* = \frac{\sigma_{21}^2}{\sigma_{21}^2+\sigma_{22}^2}\sin^2\left(\arctan\left(-\frac{\sigma_{31}}{\sigma_{33}}\right)\right)$, $\bar{k}^* = \frac{\sigma_{21}^2}{\sigma_{21}^2+\sigma_{22}^2}\sin^2\left(\arctan\left(\frac{\sigma_{33}}{\sigma_{31}}\right)\right)$ and $\sigma_{21} \geq 0$.

Assume that $\underline{k} \neq 0$, $\bar{k} \neq 1$, i.e., both lower and upper bounds in (A.21) are constrained. For $\sigma_{31} > 0$, $\bar{k} < \bar{k}^*$, $IS_\alpha(\boldsymbol{\phi})$ in (A.22) is strictly smaller than $IS_\alpha(\boldsymbol{\phi})$ in (A.19) because $\sigma_{11}\cos\left(\arcsin\left(\frac{\sqrt{\underline{k}(\sigma_{21}^2+\sigma_{22}^2)}}{\sigma_{21}}\right)\right) < \sigma_{11}$ and $\sigma_{11}\cos\left(\arcsin\left(\frac{\sqrt{\bar{k}(\sigma_{21}^2+\sigma_{22}^2)}}{\sigma_{21}}\right)\right) > \sigma_{11}\cos\left(\arctan\left(\frac{\sigma_{33}}{\sigma_{31}}\right)\right)$. For $\sigma_{31} \leq 0, \underline{k} > \underline{k}^*$, the reduction in the identified set follows from the fact that $\sigma_{11}\cos\left(\arcsin\left(\frac{\sqrt{\bar{k}(\sigma_{21}^2+\sigma_{22}^2)}}{\sigma_{21}}\right)\right) > 0$ and $\sigma_{11}\cos\left(\arcsin\left(\frac{\sqrt{\underline{k}(\sigma_{21}^2+\sigma_{22}^2)}}{\sigma_{21}}\right)\right) < \sigma_{11}\cos\left(\arctan\left(-\frac{\sigma_{31}}{\sigma_{33}}\right)\right)$. The same argument applies under $\sigma_{31} > 0, \bar{k} \geq \bar{k}^*$ and $\sigma_{31} \leq 0, \underline{k} \leq \underline{k}^*$.

Suppose that $\underline{k} = 0, \bar{k} \neq 1$, i.e., the lower bound of constraint (A.21) is unrestricted. The identified set in (A.22) then becomes

$$IS_\alpha(\boldsymbol{\phi}) \equiv \begin{cases} \left[\sigma_{11}\cos\left(\arcsin\left(\frac{\sqrt{\bar{k}(\sigma_{21}^2+\sigma_{22}^2)}}{\sigma_{21}}\right)\right), \sigma_{11}\right], \\ \text{for } \{\sigma_{31} > 0, \bar{k} < \bar{k}^*\}, \\ \left[\sigma_{11}\cos\left(\arctan\left(\frac{\sigma_{33}}{\sigma_{31}}\right)\right), \sigma_{11}\right], \\ \text{for } \sigma_{31} > 0, \bar{k} \geq \bar{k}^*, \\ \left[\sigma_{11}\cos\left(\arcsin\left(\frac{\sqrt{\bar{k}(\sigma_{21}^2+\sigma_{22}^2)}}{\sigma_{21}}\right)\right), \sigma_{11}\cos\left(\arctan\left(-\frac{\sigma_{31}}{\sigma_{33}}\right)\right)\right], \\ \text{for } \sigma_{31} \leq 0, \end{cases} \tag{A.23}$$

where $\sigma_{21} \geq 0$. For $\sigma_{31} > 0, \bar{k} \geq \bar{k}^*$, $IS_\alpha(\boldsymbol{\phi})$ in (A.23) is equivalent to $IS_\alpha(\boldsymbol{\phi})$ in (A.19); otherwise, the identified set in (A.23) is strictly smaller.

Finally, assume that $\underline{k} \neq 0, \bar{k} = 1$, i.e., the upper bound in (A.21) is unconstrained. The identified set in (A.22) is now

$$IS_\alpha(\boldsymbol{\phi}) \equiv \begin{cases} \left[\sigma_{11}\cos\left(\arctan\left(\frac{\sigma_{33}}{\sigma_{31}}\right)\right), \sigma_{11}\cos\left(\arcsin\left(\frac{\sqrt{\underline{k}(\sigma_{21}^2+\sigma_{22}^2)}}{\sigma_{21}}\right)\right)\right], \\ \text{for } \sigma_{31} > 0, \\ \left[0, \sigma_{11}\cos\left(\arcsin\left(\frac{\sqrt{\underline{k}(\sigma_{21}^2+\sigma_{22}^2)}}{\sigma_{21}}\right)\right)\right], \\ \text{for } \sigma_{31} \leq 0, \underline{k} > \underline{k}^*, \\ \left[0, \sigma_{11}\cos\left(\arctan\left(-\frac{\sigma_{31}}{\sigma_{33}}\right)\right)\right], \\ \text{for } \sigma_{31} \leq 0, \underline{k} \leq \underline{k}^*, \end{cases} \tag{A.24}$$

where $\sigma_{21} \geq 0$. For $\sigma_{31} \leq 0, \underline{k} \leq \underline{k}^*$, $IS_\alpha(\boldsymbol{\phi})$ in (A.24) is equivalent to $IS_\alpha(\boldsymbol{\phi})$ in (A.19); otherwise, the identified set in (A.24) is strictly smaller.

■

A.3 Non-Emptiness and Shrinkage

The proofs given below use the following notation and concepts. $\boldsymbol{Q} = [\boldsymbol{q}_1, \ldots, \boldsymbol{q}_n] \in \boldsymbol{\Theta}(n)$ is a $n \times n$ orthonormal matrix belonging to the space of $n \times n$ orthonormal matrices $\boldsymbol{\Theta}(n)$, where n is the number of endogenous variables in a VAR(p) model. It follows that $\boldsymbol{Q'} = \boldsymbol{Q}^{-1}$ and $\boldsymbol{q}_j \in \mathcal{R}^n$, $\boldsymbol{q}_j'\boldsymbol{q}_i = 0$ for $j \neq i$, $\sum_{j=1}^n \boldsymbol{q}_j\boldsymbol{q}_j' = \boldsymbol{I}_n$, and $||\boldsymbol{q}_j|| = 1$ for every $j \in \{1, \ldots, n\}$. $\boldsymbol{\phi} = (\boldsymbol{B}, \boldsymbol{\Sigma}) \in \boldsymbol{\Phi}$ collects the reduced-form parameters and $\boldsymbol{\Phi} \subset \mathcal{R}^{n+n^2p} \times \boldsymbol{\Xi}$, where $\boldsymbol{\Xi}$ is the space of $n \times n$ symmetric positive semidefinite matrices; see Section 2.1 in the main text for definition of $\boldsymbol{B}$ and $\boldsymbol{\Sigma}$. The domain of $\boldsymbol{\Phi}$ is restricted such that the VAR(p) is invertible into a VMA(∞). $g_{ij}^h(\boldsymbol{\phi}, \boldsymbol{Q}) \equiv \boldsymbol{e}_i'\boldsymbol{C}_h(\boldsymbol{B})\boldsymbol{\Sigma}_{tr}\boldsymbol{Q}\boldsymbol{e}_j \equiv \boldsymbol{c}_{ih}'(\boldsymbol{\phi})\boldsymbol{q}_j \in \mathcal{R}$ is the $(i, j)-$th element of $\boldsymbol{IR}^h$ for $i, j \in \{1, \ldots, n\}$ and $h = 0, 1, \ldots$.

Let $\boldsymbol{\mathcal{Q}}(\boldsymbol{\phi}|\boldsymbol{F}, \boldsymbol{S}, \boldsymbol{\Gamma})$ denote the set of $\boldsymbol{Q}$'s that satisfy sign normalizations, zero restrictions (2.5), sign restrictions (2.7), and restrictions on the FEVD (3.4); let $\boldsymbol{F}, \boldsymbol{S}, \boldsymbol{\Gamma}$ denote a short-hand notation for zero restrictions, sign restrictions, constraints on the FEVD, respectively. $IS_g(\boldsymbol{\phi}|\boldsymbol{F}, \boldsymbol{S}, \boldsymbol{\Gamma}) = \{g_{ij}^h(\boldsymbol{\phi}, \boldsymbol{Q}) : \boldsymbol{Q} \in \boldsymbol{\mathcal{Q}}(\boldsymbol{\phi}|\boldsymbol{F}, \boldsymbol{S}, \boldsymbol{\Gamma})\}$ is the identified set for the object of interest, defined as a set-valued map from $\boldsymbol{\phi}$ to a subset in $\mathcal{R}$ that delivers the range of $g_{ij}^h(\boldsymbol{\phi}, \boldsymbol{Q})$ when $\boldsymbol{Q}$ varies over $\boldsymbol{\mathcal{Q}}(\boldsymbol{Q}|\boldsymbol{F}, \boldsymbol{S}, \boldsymbol{\Gamma})$. Let f_j represent the number of zero restrictions constraining $\boldsymbol{q}_j$; $\mathcal{I}_\mathcal{S} \subset \{1, 2, \ldots, n\}$ is the set of indices such that $j \in \mathcal{I}_\mathcal{S}$ if some of the impulse responses to the j-th structural shock are sign-constrained; $\mathcal{I}_{FEV}$ is a set of indices such that $j \in I_{FEV}$ if shock j is restricted as in (3.4).

Let $\boldsymbol{\Upsilon}_S^z(\boldsymbol{\phi}) = \frac{\boldsymbol{\Upsilon}^z(\boldsymbol{\phi})+(\boldsymbol{\Upsilon}^z(\boldsymbol{\phi}))'}{2}$ denote the symmetric part of $\boldsymbol{\Upsilon}^z(\boldsymbol{\phi})$, where $z \in \Lambda_j$; $\lambda_{l,j}^z$ for $l = \{1, \ldots, n\}$ are the n real eigenvalues of $\boldsymbol{\Upsilon}_S^z(\boldsymbol{\phi})$. Note that $\lambda_{max,j}^z = max\{\lambda_{1,j}^z, \ldots, \lambda_{n,j}^z\}$

and $\lambda^z_{min,j} = min\{\lambda^z_{1,j}, \dots, \lambda^z_{n,j}\}$. Finally, let $\tilde{\boldsymbol{q}}$ be the eigenvector associated to $\lambda^z_{l,j}$, namely $\boldsymbol{\Upsilon}^z_S(\boldsymbol{\phi})\tilde{\boldsymbol{q}} = \lambda^z_{l,j}\tilde{\boldsymbol{q}}$.

Proof of Proposition 3.4.

Under $\mathcal{I}_{FEV} = \{j^*\}$, the whole set of restrictions on the FEVD is reduced to

$$\underline{k}^z_{j^*} \leq \boldsymbol{q}'_{j^*}\boldsymbol{\Upsilon}^z(\boldsymbol{\phi})\boldsymbol{q}_{j^*} \leq \bar{k}^z_{j^*} \text{ for } z \in \Lambda_{j^*}. \tag{A.25}$$

$\boldsymbol{\Upsilon}^z(\boldsymbol{\phi})$ is a positive semidefinite $n \times n$ real matrix and, as such, can be decomposed into its symmetric and antisymmetric part:

$$\boldsymbol{\Upsilon}^z(\boldsymbol{\phi}) \equiv \boldsymbol{\Upsilon}^z_S(\boldsymbol{\phi}) + \boldsymbol{\Upsilon}^z_{AS}(\boldsymbol{\phi}),$$

where $\boldsymbol{\Upsilon}^z_S(\boldsymbol{\phi}) = \frac{\boldsymbol{\Upsilon}^z(\boldsymbol{\phi})+(\boldsymbol{\Upsilon}^z(\boldsymbol{\phi}))'}{2}$ and $\boldsymbol{\Upsilon}^z_{AS}(\boldsymbol{\phi}) = \frac{\boldsymbol{\Upsilon}^z(\boldsymbol{\phi})-(\boldsymbol{\Upsilon}^z(\boldsymbol{\phi}))'}{2}$. This implies the following:

$$\begin{aligned}
\boldsymbol{q}'_{j^*}\boldsymbol{\Upsilon}^z(\boldsymbol{\phi})\boldsymbol{q}_{j^*} &= \\
\boldsymbol{q}'_{j^*}\left(\boldsymbol{\Upsilon}^z_S(\boldsymbol{\phi}) + \boldsymbol{\Upsilon}^z_{AS}(\boldsymbol{\phi})\right)\boldsymbol{q}_{j^*} &= \\
\boldsymbol{q}'_{j^*}\left(\frac{\boldsymbol{\Upsilon}^z(\boldsymbol{\phi})+(\boldsymbol{\Upsilon}^z(\boldsymbol{\phi}))'}{2} + \frac{\boldsymbol{\Upsilon}^z(\boldsymbol{\phi})-(\boldsymbol{\Upsilon}^z(\boldsymbol{\phi}))'}{2}\right)\boldsymbol{q}_{j^*} &= \\
\boldsymbol{q}'_{j^*}\left(\frac{\boldsymbol{\Upsilon}^z(\boldsymbol{\phi})+(\boldsymbol{\Upsilon}^z(\boldsymbol{\phi}))'}{2}\right)\boldsymbol{q}_{j^*} + \boldsymbol{q}'_{j^*}\left(\frac{\boldsymbol{\Upsilon}^z(\boldsymbol{\phi})-(\boldsymbol{\Upsilon}^z(\boldsymbol{\phi}))'}{2}\right)\boldsymbol{q}_{j^*} &= \\
\boldsymbol{q}'_{j^*}\left(\frac{\boldsymbol{\Upsilon}^z(\boldsymbol{\phi})+(\boldsymbol{\Upsilon}^z(\boldsymbol{\phi}))'}{2}\right)\boldsymbol{q}_{j^*} &= \\
\boldsymbol{q}'_{j^*}\boldsymbol{\Upsilon}^z_S(\boldsymbol{\phi})\boldsymbol{q}_{j^*}& \\
\text{for } z \in \Lambda_{j^*},&
\end{aligned} \tag{A.26}$$

where the second last equality comes from the fact that $\boldsymbol{q}'_{j^*}\left(\frac{\boldsymbol{\Upsilon}^z(\boldsymbol{\phi})-(\boldsymbol{\Upsilon}^z(\boldsymbol{\phi}))'}{2}\right)\boldsymbol{q}_{j^*} = 0$. Thus, restrictions (A.25) can be written as

$$\underline{k}^z_{j^*} \leq \boldsymbol{q}'_{j^*}\boldsymbol{\Upsilon}^z_S(\boldsymbol{\phi})\boldsymbol{q}_{j^*} \leq \bar{k}^z_{j^*} \text{ for } z \in \Lambda_{j^*}, \tag{A.27}$$

where $\boldsymbol{\Upsilon}^z_S(\boldsymbol{\phi}) = \frac{\boldsymbol{\Upsilon}^z(\boldsymbol{\phi})+(\boldsymbol{\Upsilon}^z(\boldsymbol{\phi}))'}{2}$.

$\boldsymbol{\Upsilon}^z_S(\boldsymbol{\phi})$ is symmetric and, as such, can be diagonalized; thus, there must exist an orthogonal matrix $\boldsymbol{P}$ such that

$$\boldsymbol{P}'\boldsymbol{\Upsilon}^z_S(\boldsymbol{\phi})\boldsymbol{P} = \boldsymbol{D}^z,$$

where $\boldsymbol{D}^z$ is a diagonal matrix

$$\boldsymbol{D}^z = \begin{bmatrix} \lambda^z_{1,j^*} & 0 & \dots & 0 \\ 0 & \lambda^z_{2,j^*} & \dots & 0 \\ \vdots & \dots & \ddots & \vdots \\ 0 & 0 & \dots & \lambda^z_{n,j^*} \end{bmatrix}$$

and diagonal entries $\lambda^z_{1,j^*}, \ldots, \lambda^z_{n,j^*}$ are real eigenvalues of $\boldsymbol{\Upsilon}^z_S(\boldsymbol{\phi})$.

Suppose that the $n \times 1$ orthogonal eigenvector associated to a specific $\lambda^z_{l,j^*} \in \{\lambda^z_{1,j^*}, \ldots, \lambda^z_{n,j^*}\}$ is $\tilde{\boldsymbol{q}}$:

$$\boldsymbol{\Upsilon}^z_S(\boldsymbol{\phi})\tilde{\boldsymbol{q}} = \lambda^z_{l,j^*}\tilde{\boldsymbol{q}} \tag{A.28}$$

It follows that

$$\tilde{\boldsymbol{q}}'\boldsymbol{\Upsilon}^z_S(\boldsymbol{\phi})\tilde{\boldsymbol{q}} = \lambda^z_{l,j^*}\tilde{\boldsymbol{q}}'\tilde{\boldsymbol{q}} = \lambda^z_{l,j^*}, \tag{A.29}$$

where the last equality comes from the fact that $\tilde{\boldsymbol{q}}'\tilde{\boldsymbol{q}} = 1$ by construction. Combining (A.26) and (A.29) yields

$$\tilde{\boldsymbol{q}}'\boldsymbol{\Upsilon}^z(\boldsymbol{\phi})\tilde{\boldsymbol{q}} = \lambda^z_{l,j^*}. \tag{A.30}$$

If $\underline{k}^z_{j^*} \leq \lambda^z_{l,j^*} \leq \bar{k}^z_{j^*}$ (condition (a)), constraint $\underline{k}^z_{j^*} \leq \boldsymbol{q}'_{j^*}\boldsymbol{\Upsilon}^z(\boldsymbol{\phi})\boldsymbol{q}_{j^*} \leq \bar{k}^z_{j^*}$ is then satisfied for $\boldsymbol{q}_{j^*} = \tilde{\boldsymbol{q}}$. Under condition (b), $\tilde{\boldsymbol{q}}$ satisfies remaining bounds on the FEVD, zero restrictions, and sign restrictions. This implies that there must exist a matrix $\tilde{\boldsymbol{Q}} = [\boldsymbol{q}_1, \ldots, \tilde{\boldsymbol{q}}, \ldots, \boldsymbol{q}_n] \in \boldsymbol{\mathcal{Q}}(\boldsymbol{\phi}|\boldsymbol{F}, \boldsymbol{S}, \boldsymbol{\Gamma})$. In turn, this leads to $\boldsymbol{\mathcal{Q}}(\boldsymbol{\phi}|\boldsymbol{F}, \boldsymbol{S}, \boldsymbol{\Gamma}) \neq \emptyset$. Given the map between the impulse response identified set $IS_g(\boldsymbol{\phi}|\boldsymbol{F}, \boldsymbol{S}, \boldsymbol{\Gamma})$ and $\boldsymbol{\mathcal{Q}}(\boldsymbol{\phi}|\boldsymbol{F}, \boldsymbol{S}, \boldsymbol{\Gamma})$, $IS_g(\boldsymbol{\phi}|\boldsymbol{F}, \boldsymbol{S}, \boldsymbol{\Gamma}) \neq \emptyset$ for every $i, j^*, z, z^* \in \{1, \ldots, n\}$ and $h = 0, 1, \ldots$. Since $|g^h_{ij^*}| \leq ||\boldsymbol{c}_{ih}(\boldsymbol{\phi})|| < \infty$ for any $i \in \{1, \ldots, n\}$, $j^* \in \{1, \ldots, n\}$, and $h = 0, 1, \ldots$, where $||\boldsymbol{c}_{ih}(\boldsymbol{\phi})||$ is bounded due to the restriction on $\boldsymbol{\phi}$ such that reduced-form VAR is invertible to VMA(∞), the boundedness of the identified set follows.

■

Proof of Proposition 3.5.

This proof greatly builds on the arguments used above. Specifically, it shows that if $\nexists z \in \Lambda_{j^*} \mid \lambda^z_{min,j^*} < \underline{k}^z_{j^*}$ or $\lambda^z_{max,j^*} > \bar{k}^z_{j^*} \Rightarrow IS_g(\boldsymbol{\phi}|\boldsymbol{F}, \boldsymbol{S}, \boldsymbol{\Gamma}) \equiv IS_g(\boldsymbol{\phi}|\boldsymbol{F}, \boldsymbol{S})$. This is equivalent to prove Proposition 3.5.

From the previous proof, it is easy to see that

$$\lambda^z_{min,j^*} \leq \boldsymbol{q}'_{j^*}\boldsymbol{\Upsilon}^z(\boldsymbol{\phi})\boldsymbol{q}_{j^*} \leq \lambda^z_{max,j^*} \text{ for } z \in \Lambda_{j^*}. \tag{A.31}$$

If $\nexists z \in \Lambda_{j^*} \mid \lambda^z_{min,j^*} < \underline{k}^z_{j^*}$ or $\lambda^z_{max,j^*} > \bar{k}^z_{j^*}$, then

$$\max_{q^*_j} \boldsymbol{q}'_{j^*}\boldsymbol{\Upsilon}^z(\boldsymbol{\phi})\boldsymbol{q}_{j^*} \leq \bar{k}^z_{j^*} \ \forall z \in \Lambda_{j^*} \tag{A.32}$$

and

$$\min_{q^*_j} \boldsymbol{q}'_{j^*}\boldsymbol{\Upsilon}^z(\boldsymbol{\phi})\boldsymbol{q}_{j^*} \geq \underline{k}^z_{j^*} \ \forall z \in \Lambda_{j^*}. \tag{A.33}$$

As a result, $\boldsymbol{\mathcal{Q}}(\boldsymbol{\phi}|\boldsymbol{F},\boldsymbol{S}) \equiv \boldsymbol{\mathcal{Q}}(\boldsymbol{\phi}|\boldsymbol{F},\boldsymbol{S},\boldsymbol{\Gamma})$; in turn, this leads to $IS_g(\boldsymbol{\phi}|\boldsymbol{F},\boldsymbol{S},\boldsymbol{\Gamma}) \equiv IS_g(\boldsymbol{\phi}|\boldsymbol{F},\boldsymbol{S})$. Proposition 3.5 follows.

■

A.4 Convexity

Proof of Proposition 3.6.

Under condition (a), the whole set of identifying assumptions is

$$\boldsymbol{S}_{j^*}(\boldsymbol{\phi})\boldsymbol{q}_{j^*} \geq \boldsymbol{0}, \tag{A.34}$$

$$\boldsymbol{q}'_{j^*}\boldsymbol{\Upsilon}^z(\boldsymbol{\phi})\boldsymbol{q}_{j^*} \leq \bar{k}^z_{j^*} \text{ for any } z \in \Lambda_{j^*}, \tag{A.35}$$

where (A.35) comes from $\underline{k}^z_{j^*} = 0$ for any $z \in \Lambda_{j^*}$. The set $\{\boldsymbol{q}_{j^*} \in \mathcal{R}^n | \boldsymbol{q}'_{j^*}\boldsymbol{\Upsilon}^z(\boldsymbol{\phi})\boldsymbol{q}_{j^*} \leq \bar{k}^z_{j^*}\ \forall z \in \Lambda_{j^*}\}$ defined by constraint (A.35) is convex because by construction $\boldsymbol{\Upsilon}^z(\boldsymbol{\phi})$ is positive semi-definite. Restrictions (A.34) impose linear constraints on $\boldsymbol{q}_{j^*}$and, as such, $\{\boldsymbol{q}_{j^*} \in \mathcal{R}^n | \boldsymbol{S}_{j^*}(\boldsymbol{\phi})\boldsymbol{q}_{j^*} \geq \boldsymbol{0},\ ||\boldsymbol{q}_{j^*}|| = 1\}$ is a convex set (Giacomini and Kitagawa, 2018). Since the intersection of convex sets is always convex, the intersection between the unit circle defined by $\boldsymbol{q}_{j^*}$ (remark: $||\boldsymbol{q}_{j^*}|| = 1$) and the sets induced by restrictions (A.34) and (A.35) determines a convex set: $\{\boldsymbol{q}_{j^*} \in \mathcal{R}^n | \boldsymbol{S}_{j^*}(\boldsymbol{\phi})\boldsymbol{q}_{j^*} \geq \boldsymbol{0},\ \boldsymbol{q}'_{j^*}\boldsymbol{\Upsilon}^z(\boldsymbol{\phi})\boldsymbol{q}_{j^*} \leq \bar{k}^z_{j^*}\ \forall z \in \Lambda_{j^*},\ ||\boldsymbol{q}_{j^*}|| = 1\}$ is convex.

Focus now on condition (b) and suppose that $\tilde{h} = 0$. First, let us derive how bounds on the FEVD can be written. From Section 3, for any $z \in \Lambda_{j^*}$

$$\boldsymbol{\Upsilon}^z(\boldsymbol{\phi}) = \frac{\sum_{h=0}^{\tilde{h}} \boldsymbol{c}_{zh}(\boldsymbol{\phi})\boldsymbol{c}'_{zh}(\boldsymbol{\phi})}{\sum_{h=0}^{\tilde{h}} \boldsymbol{c}'_{zh}(\boldsymbol{\phi})\boldsymbol{c}_{zh}(\boldsymbol{\phi})}. \tag{A.36}$$

Since $\tilde{h} = 0$,

$$\boldsymbol{\Upsilon}^z(\boldsymbol{\phi}) = \frac{\boldsymbol{c}_{z0}(\boldsymbol{\phi})\boldsymbol{c}'_{z0}(\boldsymbol{\phi})}{\boldsymbol{c}'_{z0}(\boldsymbol{\phi})\boldsymbol{c}_{z0}(\boldsymbol{\phi})}. \tag{A.37}$$

This implies that

$$\begin{aligned}
\boldsymbol{q}'_{j^*}\boldsymbol{\Upsilon}^z(\boldsymbol{\phi})\boldsymbol{q}_{j^*} &= \boldsymbol{q}'_{j^*}\frac{\boldsymbol{c}_{z0}(\boldsymbol{\phi})\boldsymbol{c}'_{z0}(\boldsymbol{\phi})}{\boldsymbol{c}'_{z0}(\boldsymbol{\phi})\boldsymbol{c}_{z0}(\boldsymbol{\phi})}\boldsymbol{q}_{j^*} \\
&= m(\boldsymbol{\phi})\boldsymbol{q}'_{j^*}\boldsymbol{c}_{z0}(\boldsymbol{\phi})\boldsymbol{c}'_{z0}(\boldsymbol{\phi})\boldsymbol{q}_{j^*} \\
&= m(\boldsymbol{\phi})(\boldsymbol{c}'_{z0}(\boldsymbol{\phi})\boldsymbol{q}_{j^*})^2,
\end{aligned} \tag{A.38}$$

where the second equality comes from the fact that $m(\boldsymbol{\phi}) = \frac{1}{\boldsymbol{c}'_{z0}(\boldsymbol{\phi})\boldsymbol{c}_{z0}(\boldsymbol{\phi})}$ is a positive scalar; the last equality derives from $\boldsymbol{q}'_{j^*}\boldsymbol{c}_{z0}(\boldsymbol{\phi}) = (\boldsymbol{q}'_{j^*}\boldsymbol{c}_{z0}(\boldsymbol{\phi}))' = \boldsymbol{c}'_{z0}(\boldsymbol{\phi})\boldsymbol{q}_{j^*}$. As a result, the whole set of constraints on the FEVD is reduced to

$$\underline{k}^z_{j^*} \leq m(\boldsymbol{\phi})(\boldsymbol{c}'_{z0}(\boldsymbol{\phi})\boldsymbol{q}_{j^*})^2 \leq \bar{k}^z_{j^*} \text{ for } z \in \Lambda_{j^*}. \tag{A.39}$$

Condition (b) also establishes that for any variable $z \in \Lambda_{j^*}$ subject to bounds on the FEV up to horizon $\tilde{h}$, responses $g^h_{zj^*}(\boldsymbol{\phi}, \boldsymbol{Q})$ are sign-restricted for $h = 0, \ldots, \tilde{h}$. Since $g^h_{zj^*}(\boldsymbol{\phi}, \boldsymbol{Q}) = \boldsymbol{c'_{zh}}(\boldsymbol{\phi})\boldsymbol{q}_{j^*}$ and $\tilde{h} = 0$, this implies

$$\boldsymbol{c'_{z0}}(\boldsymbol{\phi})\boldsymbol{q}_{j^*} \geq 0 \text{ for any } z \in \Lambda_{j^*}, \tag{A.40}$$

where, without loss of generality, it is assumed that the sign of restrictions is positive. Combining (A.39) and (A.40) shows that the whole set of bounds on the FEVD under condition (b) is reduced to some linear inequalities in $\boldsymbol{q}_{j^*}$:

$$\sqrt{\frac{\underline{k}^z_{j^*}}{m(\boldsymbol{\phi})}} \leq \boldsymbol{c'_{z0}}(\boldsymbol{\phi})\boldsymbol{q}_{j^*} \leq \sqrt{\frac{\bar{k}^z_{j^*}}{m(\boldsymbol{\phi})}}, \tag{A.41}$$

$$\boldsymbol{c'_{z0}}(\boldsymbol{\phi})\boldsymbol{q}_{j^*} \geq 0 \text{ for } z \in \Lambda_{j^*}. \tag{A.42}$$

For $\tilde{h} > 0$, a similar argument can used for proving that bounds on the FEVD can be reduced to a set of linear constraint on $\boldsymbol{q}_{j^*}$. Once the bounds on the FEVD are linearised, convexity follows.

■

B Structural Component of Monetary Policy

This Section shows how to derive coefficients of the monetary policy equation. Given the SVAR model in equation (2.1) and the monetary policy application in Section 6, without loss of generality let $\Delta y_t, \Delta c_t, \Delta I_t, \Delta w_t, l_t, \pi_t, i_t$ denote the order of variables; this implies that the monetary policy shock is the last (seventh) shock. Rewrite then the monetary policy equation as follows, abstracting from constant:

$$\boldsymbol{y'_t}\boldsymbol{A}_{0,7} = \sum_{j=1}^{p} \boldsymbol{y'_{t-j}}\boldsymbol{A}_{j,7} + \epsilon_{7,t},$$

where $\epsilon_{7,t}$ denotes the monetary policy shock, $\boldsymbol{A}_{0,7}$ and $\boldsymbol{A}_{j,7}$ represent the seventh column of $\boldsymbol{A}_0$ and $\boldsymbol{A}_j$, respectively. Restricting the systematic component of monetary policy can be reduced to impose restrictions on $\boldsymbol{A}_{j,7}$ for $j = 0, \ldots, p$. Since Arias, Caldara, and Rubio Ramírez (2018) focus on contemporaneous coefficients, let the monetary policy equation abstract from lags:

$$i_t = \gamma_{\Delta y}\Delta y_t + \gamma_{\Delta c}\Delta c_t + \gamma_{\Delta I}\Delta I_t + \gamma_{\Delta w}\Delta w_t + \gamma_l l_t + \gamma_\pi \pi_t + A^{-1}_{0,47}\epsilon_{7,t},$$

where $\gamma_{\Delta y} = A^{-1}_{0,77}A_{0,17}, \gamma_{\Delta c} = A^{-1}_{0,77}A_{0,27}, \gamma_{\Delta I} = A^{-1}_{0,77}A_{0,37}, \gamma_{\Delta w} = A^{-1}_{0,77}A_{0,47}, \gamma_l = A^{-1}_{0,77}A_{0,57}, \gamma_\pi = A^{-1}_{0,77}A_{0,67}$.

C DSGE Model

This Section of the Appendix introduces the log-linearized equations for the framework used in Section 4 of the main text.

C.1 Aggregate Demand

The resource constraint is

$$y_t = c_y c_t + i_y i_t + z_y z_t + \epsilon_t^g \tag{C.1}$$

and depends on output (y_t), consumption (c_t), investment (i_t), capital utilization costs that are a function of the capital utilization rate (z_t), and exogenous spending (ϵ_t^g). c_y, g_y, i_y denote steady-state consumption-output ratio, steady-state exogenous spending-output ratio, and steady-state investment-output ratio, respectively, where $c_y = 1 - g_y - i_y$. In turn, $i_y = (\gamma - 1 + \delta)k_y$, where γ is the steady-state growth rate, δ denotes the depreciation rate of capital and k_y represents the steady-state capital-output ratio; $z_y = R_*^k k_y$, where R_*^k denotes the steady-state rental rate of capital. Furthermore, the exogenous spending is assumed to follow an AR(1) process with an IID-Normal error term ($\eta_t^g \sim N(0, \sigma_g^2)$) augmented by a productivity shock ($\eta_t^a \sim N(0, \sigma_a^2)$): $\epsilon_t^g = \rho_g \epsilon_{t-1}^g + \eta_t^g + \rho_{ga}\eta_t^a$.

I derive consumption dynamics from the consumption Euler equation:

$$c_t = c_1 c_{t-1} + (1 - c_1)E_t c_{t+1} + c_2(l_t - E_t l_{t+1}) - c_3(r_t - E_t \pi_{t+1} + \epsilon_t^b), \tag{C.2}$$

where $c_1 = \frac{\lambda}{\gamma}(1 + \frac{\lambda}{\gamma}), c_2 = \frac{(\sigma_c - 1)(\frac{W_*^h L_*}{C_*})}{\sigma_c(1+\frac{\lambda}{\gamma})}, c_3 = \frac{1-\frac{\lambda}{\gamma}}{(1+\frac{\lambda}{\gamma})\sigma_c}$. It implies that current consumption depends on a (weighted) average of past and expected consumption, expected growth in hours worked (l_t), the ex-ante real interest rate and a shock element ϵ_t^b. λ denotes external habit and σ_c is the inverse of the elasticity of intertemporal substitution for consumption, or risk aversion coefficient. Note that with no external habit formation ($\lambda = 0$) and log-utility in consumption ($\sigma_c = 1$), standard merely forward-looking consumption equation is obtained. ϵ_t^b is a risk premium term and follows an AR(1) process with an IID-Normal error term ($\eta_t^b \sim N(0, \sigma_b^2)$): $\epsilon_t^b = \rho_b \epsilon_{t-1}^b + \eta_t^b$, i.e., a shock to this element is a risk premium shock.

I derive investment dynamics from the investment Euler equation:

$$i_t = i_1 i_{t-1} + (1 - i_1)E_t i_{t+1} + i_2 q_t + \epsilon_t^i, \tag{C.3}$$

where $i_1 = \frac{1}{1+\beta\gamma^{1-\sigma_c}}, i_2 = \frac{1}{(1+\beta\gamma^{1-\sigma_c})\gamma^2\varphi}$, and q_t is the value of capital stock. φ is the steady-state elasticity of the capital adjustment cost function and β denotes the discount factor. ϵ_t^i is a disturbance term to the investment-specific technology process and follows an AR(1) process with an IID-Normal error term ($\eta_t^i \sim N(0, \sigma_i^2)$): $\epsilon_t^i = \rho_i \epsilon_{t-1}^i + \eta_t^i$.

The arbitrage equation for the value of capital is

$$q_t = q_1 E_t q_{t+1} + (1 - q_1) E_t r_{t+1}^k - (r_t - E_t \pi_{t+1} + \epsilon_t^b), \tag{C.4}$$

where $q_1 = \beta \gamma^{-\sigma_c}(1 - \delta) = \frac{1-\delta}{R_*^k + (1-\delta)}$. Thus, the value of capital stock depends on its expected value, the expected real rental rate on capital, the ex-ante real interest rate, and the risk premium disturbance.

C.2 Aggregate Supply

The production function is

$$y_t = \phi_p(\alpha k_t^s + (1 - \alpha) l_t + \epsilon_t^\alpha), \tag{C.5}$$

where inputs of production are capital services (k_t^s) and hours worked. TFP (ϵ_t^α) follows an AR(1) process with an IID-Normal error term ($\eta_t^a \sim N(0, \sigma_a^2)$): $\epsilon_t^a = \rho_a \epsilon_{t-1}^a + \eta_t^a$. The share of capital in production is denoted by α, while ϕ_p equals one plus the share of fixed costs in production (Φ).

The current capital services used as input in production are a function of capital installed in the previous period (k_{t-1}) and the degree of capital utilization (z_t):

$$k_t^s = k_{t-1} + z_t. \tag{C.6}$$

Cost minimization by the households that give capital services leads to the following equilibrium condition for the capital utilization:

$$z_t = z_1 r_t^k, \tag{C.7}$$

where $z_1 = \frac{1-\psi}{\psi}$ and ψ denotes a positive function of the elasticity of capital utilization adjustment cost function. It is normalized such that $\psi \in [0, 1]$. $\psi = 1$ implies that it is very costly to change the utilization of capital and the latter remains unchanged. On the other hand, if $\psi = 0$, the marginal cost of changing the utilization of capital does not move and the rental rate on capital is constant in equilibrium.

The following equation delivers the accumulation of installed capital (k_t), which depends on the flow of investment and an investment-specific technology disturbance:

$$k_t = k_1 k_{t-1} + (1 - k_1) i_t + k_2 \epsilon_t^i, \tag{C.8}$$

where $k_1 = \frac{1-\delta}{\gamma}$ and $k_2 = (1 - \frac{1-\delta}{\gamma})(1 + \beta \gamma^{1-\sigma_c})\gamma^2 \delta$.

In the monopolistic competitive goods market, firms minimize costs and, as a result, the price mark-up (μ_t^p), which is the difference between the average price and the nominal marginal costs, equals the difference between the marginal product of labour (mpl_t) and the real wage (w_t):

$$\mu_t^p = mpl_t - w_t = \alpha(k_t^s - l_t) + \epsilon_t^a - w_t. \tag{C.9}$$

Maximization of profit by firms yields the following Phillips curve:

$$\pi_t = \pi_1 \pi_{t-1} + \pi_2 E_t \pi_{t+1} - \pi_3 \mu_t^p + \epsilon_t^p, \tag{C.10}$$

with $\pi_1 = \frac{\iota_p}{1+\beta\gamma^{1-\sigma_c}\iota_p}$, $\pi_2 = \frac{\beta\gamma^{1-\sigma_c}}{1+\beta\gamma^{1-\sigma_c}\iota_p}$, and $\pi_3 = \frac{1}{1+\beta\gamma^{1-\sigma_c}\iota_p}\frac{(1-\beta\gamma^{1-\sigma_c}\xi_p)(1-\xi_p)}{\xi_p((\phi_p-1)\epsilon_p+1)}$. ι_p and ξ_p denote the degree of indexation to past inflation and the degree of price stickiness, respectively; ϵ_p is the curvature of the Kimball goods market aggregator. Thus, inflation (π_t) is a positive function of past and expected inflation, and of mark-up disturbance (ϵ_t^p); it is negatively affected by current price mark-up. The price mark-up disturbance follows an ARMA(1,1) with an IID-Normal error term ($\eta_t^p \sim N(0, \sigma_p^2)$): $\epsilon_t^p = \rho_p \epsilon_{t-1}^p + \eta_t^p - \mu_p \eta_{t-1}^p$. The MA element captures the high frequency movements in inflation. Depending on the degree of indexation and stickiness, prices may adjust slowly to the mark-up. Furthermore, such an adjustment is also affected by the curvature of the Kimball goods market aggregator and the steady-state mark-up, which is a function of ϕ_p due to a zero-profit condition. Note that with no indexation ($\iota_p = 0$), equation above becomes a standard, merely forward-looking Phillips curve. Under flexible prices ($\xi_p = 0$) and the price mark-up shock is zero, Phillips curve delivers that the price mark-up is constant.

The rental rate of capital is negatively affected by the capital-labour ratio and positively related to the real wage:

$$r_t^k = -(k_t - l_t) + w_t, \tag{C.11}$$

where equilibrium condition above follows from minimization of costs by firms.

In the monopolistic competitive labour market, the wage mark-up (μ_t^w) equals the difference between the real wage and marginal rate of substitution between working and consuming, denoted as mrs_t:

$$\mu_t^w = w_t - mrs_t = w_t - \sigma_l l_t - \frac{1}{1-\frac{\lambda}{\gamma}}(c_t - \frac{\lambda}{\gamma} c_{t-1}), \tag{C.12}$$

where σ_l and λ denote the elasticity of labour supply with respect to real wages and the habit parameter in consumption, respectively.

Depending on the degree of indexation and wage stickiness, real wages may adjust sluggishly to the wage mark-up:

$$w_t = w_1 w_{t-1} + (1 - w_1)(E_t w_{t+1} + E_t \pi_{t+1}) - w_2 \pi_t + w_3 \pi_{t-1} - w_4 \mu_t^w + \epsilon_t^w, \tag{C.13}$$

where $w_1 = \frac{1}{1+\beta\gamma^{1-\sigma_c}}$, $w_2 = \frac{1+\beta\gamma^{1-\sigma_c}\iota_w}{1+\beta\gamma^{1-\sigma_c}}$, $w_3 = \frac{\iota_w}{1+\beta\gamma^{1-\sigma_c}}$ and $w_4 = \frac{1}{1+\beta\gamma^{1-\sigma_c}} \frac{(1-\beta\gamma^{1-\sigma_c}\xi_w)(1-\xi_w)}{\xi_w(\phi_w-1)\epsilon_w+1}$. ι_w and ξ_w denote the degree of indexation to past inflation and the degree of wage stickiness, respectively; ϵ_w is the curvature of the Kimball labour market aggregator. Thus, real wages (w_t) are affected by past and expected real wages, current, past and expected inflation, wage mark-up, and a wage-mark up disturbance (ϵ_t^w). The latter follows an ARMA(1,1) process with an IID-Normal error term ($\eta_t^w \sim N(0, \sigma_w^2)$): $\epsilon_t^w = \rho_w \epsilon_{t-1}^w + \eta_t^w - \mu_w \eta_{t-1}^w$. The MA element captures the high frequency movements in wages. Depending on the degree of indexation and stickiness, real wages may adjust gradually to the mark-up. Furthermore, such an adjustment is also affected by the demand elasticity for labour, which is a function of the steady-state labour market mark-up ($\phi_w - 1$) and the curvature of the Kimball labor market aggregator. Note that with no indexation ($\iota_w = 0$), real wages are not affected by past inflation. Under flexible wages ($\xi_w = 0$), the real wages are a constant mark-up over the marginal rate of substitution between working and consuming.

Finally, the equation below presents the monetary policy reaction function:

$$r_t = \rho r_{t-1} + (1-\rho)[r_\pi \pi_t + r_Y(y_t - y_t^p)] + r_{\Delta y}[(y_t - y_t^p) - (y_{t-1} - y_{t-1}^p] + \epsilon_t^r. \qquad \text{(C.14)}$$

The central bank follows a Taylor rule by adjusting the policy interest rate (r_t) to inflation and output gap ($y_t - y_t^p$), namely the difference between actual and potential output.[17] ρ denotes the degree of interest rate smoothing; $r_{\Delta y}$ captures the effect of short-run variation in the output gap. ϵ_t^r is the monetary policy shocks and follows an AR(1) process with an IID-Normal error term ($\eta_t^r \sim N(0, \sigma_r^2)$): $\epsilon_t^r = \rho_r \epsilon_{t-1}^r + \eta_t^r$.

[17] The potential output is the level of output under flexible wages and prices, and without mark-up shocks.